Virtual laser scanning of dynamic scenes (VLS-4D): Current approaches and future perspectives in remote sensing

Hannah Weiser[a, b], Bernhard Höfle[a, b]

[a]3DGeo Research Group, Institute of Geography, Heidelberg University. Im Neuenheimer Feld 368. Heidelberg, 69120, Baden-Württemberg, Germany, h.weiser@uni-heidelberg.de.

[b]Interdisciplinary Center for Scientific Computing (IWR), Heidelberg University, Im Neuenheimer Feld 205, Heidelberg, 69120, Baden-Württemberg, Germany, hoefle@uni-heidelberg.de.

This manuscript is a non-peer-reviewed preprint and has been submitted for publication in *ISPRS Journal of Photogrammetry and Remote Sensing*.

Graphical Abstract

Virtual laser scanning of dynamic scenes (VLS-4D): Current approaches and future perspectives in remote sensing

Hannah Weiser, Bernhard Höfle

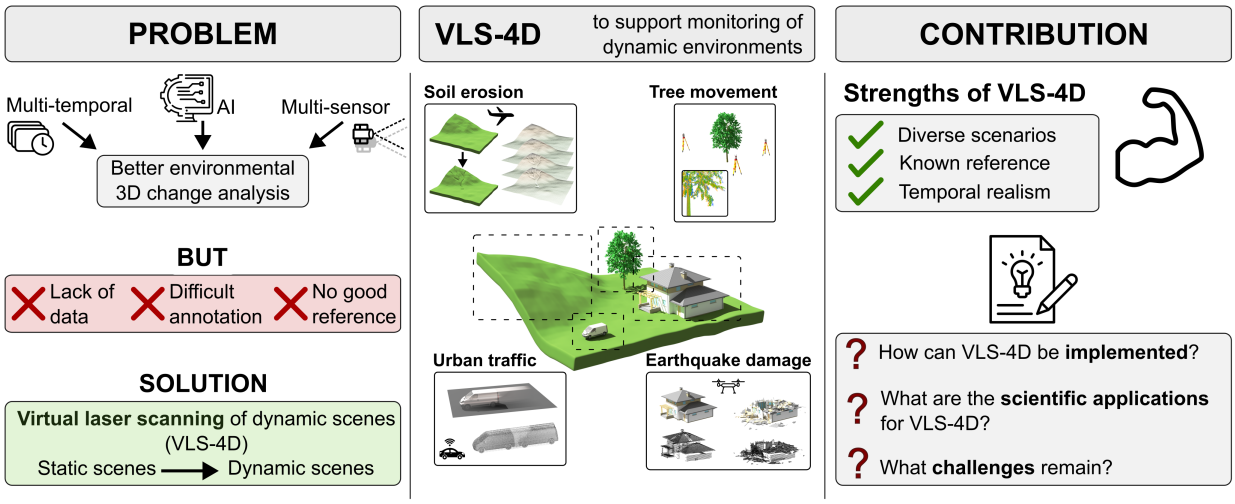

Virtual laser scanning of dynamic scenes (VLS-4D): Current approaches and future perspectives in remote sensing

Hannah Weiser[a,b], Bernhard Höfle[a,b]

[a] *3DGeo Research Group, Institute of Geography, Heidelberg University, Im Neuenheimer Feld 368, Heidelberg, 69120, Baden-Württemberg, Germany*
[b] *Interdisciplinary Center for Scientific Computing (IWR), Heidelberg University, Im Neuenheimer Feld 205, Heidelberg, 69120, Baden-Württemberg, Germany*

Abstract

Virtual laser scanning (VLS) has proven to be a useful tool for survey planning, method development and training data generation in a variety of areas of Earth and environmental sciences. Until recently, most applications have used static representations of the real or a fictive environment, neglecting the inherent dynamics of our world, that also affect Light Detection and Ranging (LiDAR) measurements.

Given the enormous potential of LiDAR simulation to support the monitoring of dynamic phenomena such as landslides, tree sway or urban change, this review provides an overview of current approaches to virtual laser scanning of dynamic scenes (VLS-4D). We first build a theoretical framework that includes the relevant types of changes to scene objects and the strategies by which they are implemented in the simulation. Furthermore, we review methods for generating dynamic scenes as input to VLS, present existing frameworks supporting VLS-4D, and highlight the main scientific objectives of the VLS-4D studies published so far. Despite the established use of VLS-4D in robotics and autonomous driving, there are few examples in environmental science where high fidelity is required not only of the scene and its dynamics, but also of the simulated ray-scene interaction.

With our work, we aim to direct future research and encourage geoscientific disciplines to adopt VLS-4D as an environment for experimentation, method development and data generation and permutation.

Keywords: Virtual LiDAR, LiDAR simulation, 3D animation, change analysis,

multi-temporal point clouds, synthetic training data

1. Introduction

Swaying trees, urban traffic, natural hazards: Monitoring such dynamic phenomena in high resolution requires multi-temporal 3D observations, particularly those based on laser scanning. To process and analyse the resulting point clouds, 3D and 4D (3D space + time) algorithms are continuously being developed and improved (Eitel et al., 2016). Thanks to improvements in computing infrastructure and the rise of machine learning (ML) and deep learning (DL), many tasks such as point cloud classification and 3D change analysis can be automated. However, lack of labelled point cloud data for training and validation is often hindering or slowing scientific and methodological progress (de Gélis et al., 2023b; Wang et al., 2023b).

Repeated laser scanning acquisition is costly and few open multi-temporal, annotated and quality-controlled datasets exist (Eitel et al., 2016; Kharroubi et al., 2022). Furthermore, collection of reference data and manual annotation of point clouds and their dynamics is tedious and sometimes not feasible at all. By now, many annotated real datasets exist for tasks on mono-temporal point clouds such as segmentation (e.g., Hessigheim3D; Kölle et al., 2021, Semantic3D; Hackel et al., 2017, SemanticKITTI; Behley et al., 2019; Geiger et al., 2012, FRACTAL; Gaydon et al., 2024, FORInstance; Puliti et al., 2023) but Kharroubi et al. (2022) could identify only one real-world multi-temporal point cloud dataset[1] that also included change labels (no change, removed, added, change).

One way to overcome the lack of annotated test and training data is to complement or substitute real data with synthetic data simulated by virtual laser scanning (VLS) (Bechtold and Höfle, 2016; Esmorís et al., 2024; Gastellu-Etchegorry et al., 2016; Lohani and Mishra, 2007; Lohani et al., 2024; Winiwarter et al., 2022b). VLS is the computer simulation of realistic Light Detection and Ranging (LiDAR) applications, by modelling the behaviour of the platform , the specifications of the scanner and the interaction between the virtual

[1] `https://kutao207.github.io/`, last accessed 2024-10-02

ray and the scene (Bechtold and Höfle, 2016; Lohani and Mishra, 2007; Gastellu-Etchegorry et al., 2016; Winiwarter et al., 2022b).

The development of algorithms for both mono- and multi-temporal data can benefit from simulated laser scanning data for two important reasons: 1) Scenario building: Point cloud representations of the same object can differ drastically depending on the acquisition platform, sensor, scan settings, and object dynamics. While real data acquisition is limited by time and equipment to one or a few scenarios, VLS allows a wide range of acquisition scenarios to be covered by varying the simulation parameters. 2) Reference data: Scene and object properties that serve as reference data can be extracted directly from the virtual input scene without annotation errors (Winiwarter et al., 2022b). Such properties include semantic classes (e.g. facade, roof, tree in an urban scene), geometric attributes (e.g. stem diameter or tree height), and temporal dynamics (e.g. magnitude, direction and type of change). Typically, these reference properties are measured by hand, manually annotated, or obtained from complementary, often higher resolution measurements. This comes with the challenge of measurement synchronisation and results in errors and (unknown) ambiguities.

VLS investigates a substitute of reality by simplifying the 3D scene and the beam-scene interaction, resulting in a digital twin of real LiDAR applications. As with every simulation, different components of reality are either reduced in their level of detail or omitted altogether (Winiwarter et al., 2022b). In terms of the virtual 3D scene in laser scanning simulations, one such component is the temporal domain, i.e. how objects and surfaces change over time. In most VLS studies, the temporal component is completely neglected by using a static model of the virtual scene, like a "frozen world". For many applications, however, it is the temporal dynamics that are of primary interest. The development of methods for e.g. change detection, spatio-temporal segmentation or moving object detection, requires controlled research data from dynamic environments, which highlights the relevance of VLS of dynamic scenes (VLS-4D). We define VLS-4D as VLS where the scene is dynamic during a survey or in between multiple surveys, and where these dynamics are relevant to the beam-scene interaction that is being simulated. Relevant dynamics therefore include changes in the geometry or reflective properties of the scene (Section 2.1).

Many previous studies considering temporal dynamics have used multiple static representations, like snapshots, of a dynamic world (e.g., de Gélis et al., 2021; Wang et al., 2022; Winiwarter et al., 2022a; Zahs et al., 2023). While simple and universally applicable to different kinds of simulation frameworks, the snapshot approach only allows for the representation of changes that occur between simulation runs. Reproducing effects such as geometrically distorted cars, vehicles that appear more than once and the occlusion effects associated with them in urban mobile laser scanning (MLS) in VLS requires scene updates during the simulation and therefore specific functionality of the simulation engine.

To date, there is no general-purpose LiDAR simulator that meets all of the current requirements for VLS-4D in the field of remote sensing of the environment. In the domain of autonomous driving, there are some highly specialised LiDAR simulation frameworks with dynamic scene support such as the open-source simulator CARLA (Dosovitskiy et al., 2017) or simulators based on the video game Grand Theft Auto V (GTA-V) (Hurl et al., 2019). However, these simulation environments are limited to ground-based sensor platforms, they lack full-waveform simulation capabilities, and scenes are difficult to customise, especially beyond outdoor driving scenes. HELIOS++, an open-source general-purpose LiDAR simulator (Winiwarter et al., 2022b) includes specific functionality to simulate rigidly moving objects during the simulation, but cannot yet represent object deformations or armature animations. While BlenSor (Gschwandtner et al., 2011), a plugin integrated to the 3D creation suite Blender, allows simulations of scenes with any animation that can be created with Blender, it simplifies the ray-scene interaction by not considering reflectance of objects or divergence of the laser beam.

As we have entered the era of multi-temporal data, multi-sensor data, and artificial intelligence, the increased use of VLS-4D is foreseeable. With VLS-4D, the remote sensing community can prepare for the increasing availability of point cloud time series data acquired by different sensor systems by developing the advanced methods to analyse these current and future datasets in depth. This great potential, as well as the current limitations and challenges of VLS-4D, are the motivation for this review article.

The objectives of this work are to

1. develop a theoretical framework by defining VLS-4D and characterising its main components (Section 2);
2. provide a review and categorisation of current approaches to VLS-4D regarding scene generation, simulation frameworks and remote sensing applications (Section 3);
3. identify research gaps, challenges and future perspectives for VLS-4D (Section 4).

2. Theoretical Framework

2.1. Definition of virtual laser scanning of dynamic scenes

Virtual laser scanning (VLS) is the simulation of 3D laser scanning using models of scenes, platforms, scanners and the beam-scene interaction (Winiwarter et al., 2022b). In this work, our definition of VLS includes approaches that synthesise LiDAR point clouds based on rendering techniques such as ray tracing, rasterisation (cf. depth buffers), and also neural volume rendering. Although these techniques may use different representations of 3D scenes, the key VLS-4D concepts of change logic (Section 2.4) and simulator-scene interaction (Section 2.6) apply to all of them.

A central component of VLS is the virtual 3D scene, a smaller and simplified section of the real or a fictional world. Now what makes such a VLS scene dynamic? A dynamic scene undergoes changes that are influencing the simulated beam-scene interaction, e.g. as changes in geometrical or spectral properties (Figures 1 and 2). The changes may happen i) in between several acquisitions or epochs (Figure 1a and d), ii) in between several scans (and therefore simulation runs), which make up a single acquisition or epoch (Figure 1b: multi-station terrestrial laser scanning), or c) during a single scan (Figure 1c).

In principle, our definition of VLS-4D also includes the interaction between the dynamic scene and the virtual survey, i.e., the definition of the platform movement and the configuration of the scanner. This means that changes in the scene may affect the survey properties, e.g. the survey path is altered to avoid collision with the dynamic scene, or the scan interval or resolution are increased as the scan system detects changes in the scene. This is highly relevant for autonomous driving scenarios and permanent laser scanning setups.

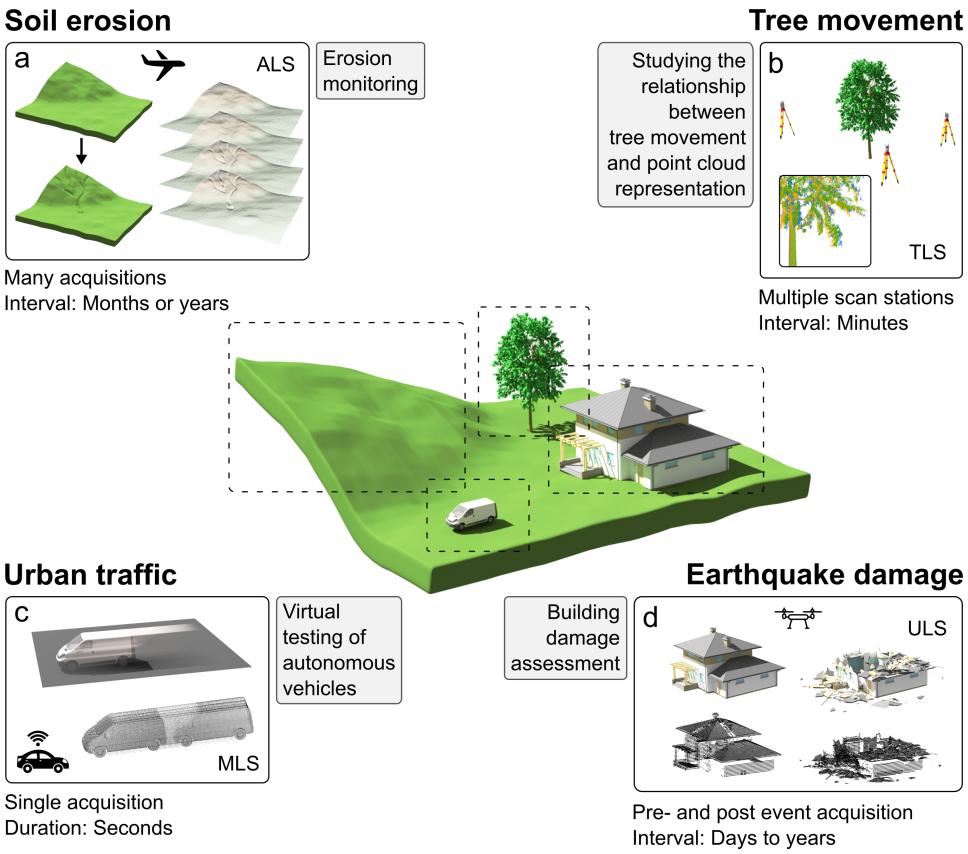

Figure 1: Schematic virtual scene with four dynamic objects. Panels (a) – (d) illustrate the examples of VLS-4D scenarios that can be simulated over each dynamic object with the resulting point clouds. Each scenario is characterised by the scientific objective (small grey boxes), the acquisition platform (abbreviations in the image boxes), the number of acquisitions and the acquisition interval or duration (below each image box). ALS = Airborne Laser Scanning, MLS = Mobile Laser Scanning, ULS = UAV-based Laser Scanning, TLS = Terrestrial Laser Scanning.

2.2. Main components of virtual laser scanning of dynamic scenes

Previous work on LiDAR simulation has defined several main components (Winiwarter et al., 2022b; Reitmann et al., 2021; Rott, 2022; Alldén et al., 2017). These include a virtual environment (scene), virtual sensors (scanners) and their settings, and the ray tracing and signal processing module. Further components, although not always explicitly mentioned, are the platform, on which the sensor is mounted, the platform trajectory, the graphical or programmatic user interface, the point cloud labelling by scene properties, and the data export. Some further optional components may be outsourced to external software, e.g. visualisation.

If dynamic scenes are to be supported explicitly in VLS software, further internal or external extensions are required and must be added to static VLS. First, a process simulation module (e.g., traffic simulation), a physics engine and/or a 3D animation module are typically used to create the virtual dynamic scene (Section 2.5). Second, the LiDAR beam-scene interaction logic must allow the scene to be updated between cast rays (Section 2.6). Third, memory handling may be optimised for dynamic scenes 4.4. Which of these extensions are required depends on the characteristics of dynamic scenes (Figure 2) and the change logic used to represent them (Figure 3), which is the topic of the following two sections.

2.3. Characteristics of dynamic virtual scenes in the context of virtual laser scanning

For the "digital twin" used as input scene for VLS-4D, the dynamics of real-world processes must be simplified while still being representative. This simplification is necessary due to incomplete knowledge of the process, to make the process easier to model and to limit the computational cost of the LiDAR simulations.

The logic suitable to represent dynamic scenes (cf. Section 2.4) depends on their characteristics and on the virtual acquisition settings that interact with them, which are summarised in Figure 2 and discussed in this section.

2.3.1. Type of change

Changes of scene objects can be related to their geometry, their material, or a combination of both. Geometric changes of objects in a scene can be categorised as rigid body

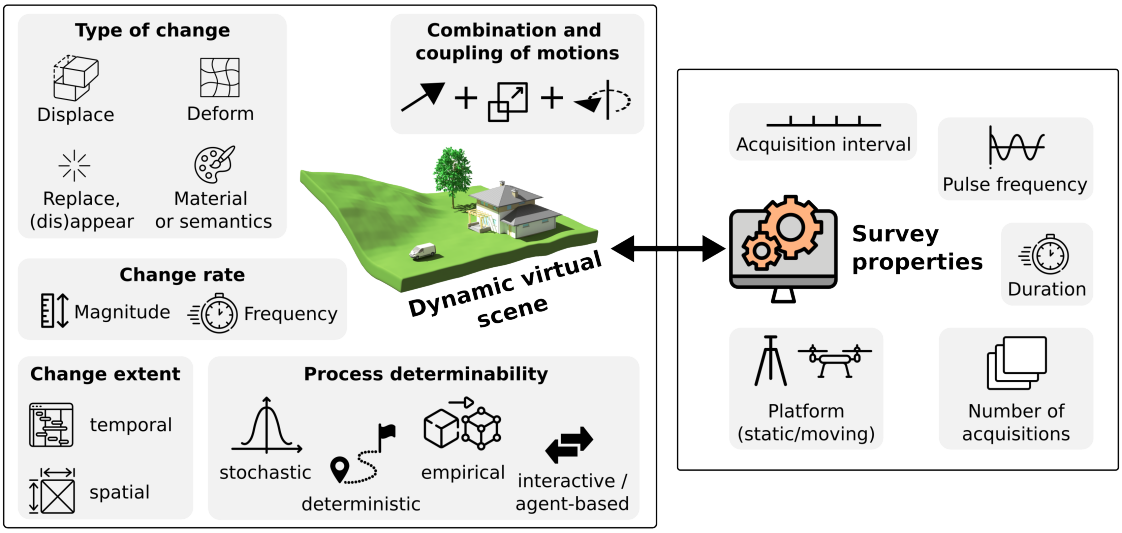

Figure 2: Characteristics of dynamic scenes and survey settings which govern how VLS-4D can or must be implemented.

displacement (e.g., cars driving on the road), deformation (e.g., vegetation movement, geomorphological surface change), or as the complete replacement, removal or addition of the objects. An example of material properties that may change are spectral properties, e.g. when modelling leaf senescence (the process of leaf ageing, including chlorophyll degradation), which will alter the backscatter intensity modelled in VLS. A change in geometry or material can also be accompanied by a change in the semantic label of the object, e.g. when a tree dies and becomes standing deadwood. VLS can also be used to label change objects and their change types themselves.

2.3.2. Change rate

Change rates of dynamic phenomena span from a few cm/year (e.g., slow landslides, tree growth) to many m/s (e.g., extremely rapid landslides, urban traffic), requiring different acquisition intervals to monitor them. An important design decision in VLS-4D is whether the scene updates should occur repeatedly during single simulation runs, as for mobile laser scanning in autonomous driving scenarios, or only between successive runs, as for repeated laser scanning of a landslide (Section 2.6). The change rates of the dynamic objects are important for choosing a suitable scene update frequency and simulation strategy

(Section 2.4).

2.3.3. Change extent

The extent of change can be described in both the temporal and spatial dimensions, where the temporal extent refers to the duration and the spatial extent refers to the size of the change object, including the initial state, the final state, and all intermediate states. The extent is important for the questions where and when a scene or part of the scene needs to be updated, depending on the position and view of the sensor (2.6).

2.3.4. Combination and coupling of motions

Dynamic objects in virtual scenes may have only their own motion, or they may be affected by the motions of other objects. Objects can inherit motions from a parent object or different motions related to different processes can be coupled. For example, we might want perform repeated LiDAR simulation over soil creep, where the surface deforms and, as a consequence, surface objects such as fences, poles and trees tilt (rigid transformation) or bend (deformation).

Dynamics may also depend on the interaction between objects. For example, rockfalls can be simulated using physics engines that take into account the collision responses of individual fragments (Sala et al., 2019).

2.3.5. Process determinability

Whether the scene dynamics can be precomputed prior to simulation or must be integral part of the simulation engine depends on their determinability. For deterministic processes, it is possible to precompute which dynamic objects will be in the field of view of a virtual sensor at what time, and therefore when they need to be updated (Section 4.4). If a deterministic dynamic scene is based on real-world observations, e.g., change obtained from a real laser scanning time series (Winiwarter et al., 2022a), we refer to it as empirical (Figure 2).

Stochastic processes require prior simulation of a possible output trajectory, so they can then be treated as deterministic processes in VLS-4D, or they require the scene update module of the simulation engine to calculate the output of each event based on random

numbers or distributions. Finally, if the dynamics depend on other simulation agents, on user input or on the data obtained by the virtual sensor, the process is agent-based or interactive and requires on-the-fly computation of the simulator (Section 2.6).

2.4. Scene change logic

In this section, we describe the three concepts with which change in VLS scenes can be implemented based on a) whether the scene is updated between repeated surveys or within a single survey and b) if the update is implemented as a new scene input from the user or handled by computations of the simulation engine. The concepts are visualised in Figure 3.

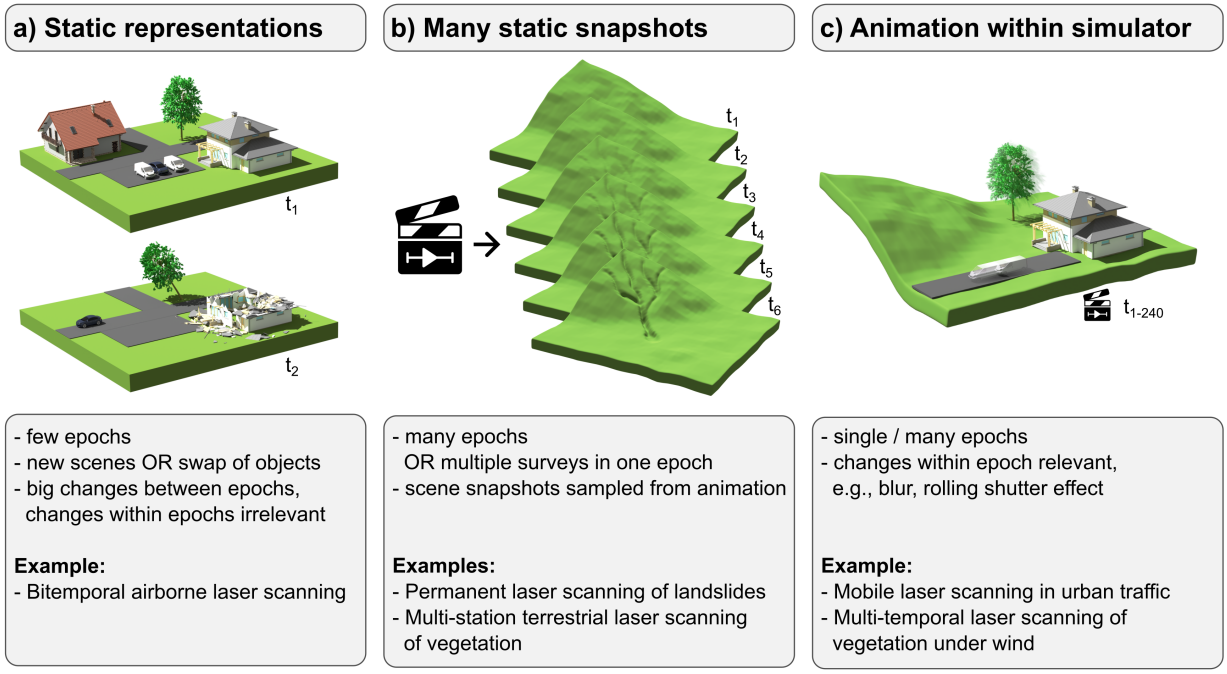

Figure 3: Overview of the three change logic concepts, their main characteristics and examples of VLS-4D scenarios for which the concepts are suitable.

2.4.1. Concept of static representations

The first approach for VLS-4D is the concept of static representations, where a simulation is executed several times over modified versions of the same scene, but the scene does not change during a single simulation run (Figure 3a). This is useful for representation of large changes after longer time spans, where smaller changes during the single acquisitions can be

neglected. These scenarios usually focus on removal, addition, replacement, or displacement of objects and do not use animation techniques to generate the scenes. Examples include simulations of bi-temporal VLS point clouds to develop methods for assessing urban change such as damage, demolition, or new construction of buildings (de Gélis et al., 2023a; Zahs et al., 2023). For each simulation run, the user can either input a completely new scene, or the simulator can handle the modification of specific parts of the scene, which we refer to as the "swap-on-repeat" feature (HELIOS++, Winiwarter et al., 2022b; BLAINDER, Reitmann et al., 2021, see Section 2.6).

2.4.2. Concept of many static snapshots

With the concept of using many static snapshots, static snapshots are sampled from a dynamic scene, which is usually animated, and used for the new simulated epoch (Figure 3b). This is useful when we want to mimic acquisitions with a short acquisition interval and a large number of epochs. An exemplary use case is multi-temporal or even permanent laser scanning (PLS) to monitor topographic surface change, as illustrated in Figure 1a (Tabernig et al., 2024).

This approach can also be used to capture changes within a single survey, by temporally subdividing simulations into many subsets. Each of these smaller subsets then uses an updated snapshot of the dynamic scene, which is usually animated. A use case for this change logic is multi-station terrestrial laser scanning (TLS), where an updated scene can be used for each scan position. When simulating multi-station TLS of vegetation (Figure 1b), this approach allows to capture wind-induced vegetation movement, resulting in different representations in scans acquired from different scan positions, introducing effects such as duplicate branches and leaves (Weiser, 2024).

2.4.3. Concept of animation within simulator

For applications where the virtual scene needs to change continuously during a single simulation run (e.g., mobile laser scanning of traffic scenarios, Figure 1c) and a large number of scene updates are required, the animation has to be integrated into the simulator (Figure

3c). This way, scene updates do not require new user input, but they are handled by the simulation engine using a defined update frequency (Section 2.6).

2.5. Animation strategies

The concepts of many static snapshots and of animation require animated scenes. With 3D computer animation, the illusion of movement is achieved by repeatedly rendering still images, called frames, of a 3D scene that is changing over time. LiDAR simulation can use the same technique, but instead of sampling an image at each time step, a series of virtual laser pulses are emitted and their returns are recorded on the "frozen" virtual scene.

In this section, we look at different ways in which scenes for VLS-4D can be animated, including interpolation between keyframes or blend shapes, control via functions or mathematical expressions, as well as physics and crowd simulation.

2.5.1. Animation with keyframes

With keyframes, the movement of the scene can be directed by defining starting, middle and ending states of objects. All frames between the keyframes (inbetweens) can be computed using different interpolation methods (Chopine, 2012, Chapter 8; Blain, 2022, Chapter 20). As an example, if we use this strategy to animate a car driving on a street, fewer keyframes are needed for a car that continues straight, more for a car that takes several turns or stops multiple times due to obstacles.

2.5.2. Skeleton animation

In VLS-4D, we might want to animate pedestrians, animals and plants. To make this realistic, we need to use rigging, the technique of skeletal animation. A rig consists of a mesh model, an armature and controls (Blain, 2022, Chapter 22). The armature is a series of bones representing the skeleton of the object and has a hierarchical structure, in which parent bones control the movement of their child bones. Typically, bones are linked to the vertices of the object mesh (skin) which deforms around the joints (Chopine, 2012, Chapter 7).

2.5.3. Sculpting, deform modifiers and shape keys

To model processes such as soil erosion or ground subsidence, the vertices of the object have to be moved to change its shape (Chopine, 2012). Modelling software provide tools for deformation such as manual sculpting or a range of automatic deform modifiers. These modifiers simplify the modification of many related vertices in a non-destructive way. Interpolation, or morphing, between shapes of an object can be achieved with shape keys (also called blend shapes or morph targets; Blender Documentation Team, 2024, Chopine, 2012, Chapter 6) which can again be animated with keyframes.

2.5.4. Data-driven animation and motion capture

If very dense capture of motion or change is available, all states (frames) of an object can be provided and exactly recreated (cf. motion capture).

2.5.5. Mathematical expressions

The motion or deformation of scene objects may also be described using mathematical expressions or functions (incl. vectors and rotation matrices) which are typically scripted. Mathematical expressions also give the option to introduce randomness.

2.5.6. Crowd simulation

For larger systems with dynamic agents (i.e., individual characters such as people or vehicles), where it is difficult to configure the dynamics of each agent individually, crowd and traffic simulation are used (Liu et al., 2020; Reynolds, 1999; Xu et al., 2014; Yang et al., 2020).

2.5.7. Physics simulation

Processes like gravitational mass movements can be modelled using physics-based simulations. Erleben et al. (2005, Chapter 1.1) explain physics-based animation as taking theoretical laws and tools from physics and mathematics, and adding "some geometry" to them to obtain mathematical models of the real world, which can be converted into numerical models and programmed on a computer. This program can then predict, where and how objects are likely to move, collide, and deform.

2.6. Interactions between the dynamic scene and the simulation engine

As introduced before, a main distinction can be made between scenes that are rebuilt between simulation runs and scenes that are changed during simulation runs. Below, we present how these scenes are interacting with the simulation engine and how memory management and performance can be optimised. For the case of rebuild during the simulation, the update frequency is discussed in more detail.

2.6.1. Full rebuild of scenes

In order to improve overall simulation performance for the concepts of static representations or static snapshots (Section 2.4), the scene can be divided into the static background and the dynamic objects, and only the dynamic objects are rebuilt for new simulation runs. Several studies have used similar approaches of composing the scene from a static background scene or "map", often obtained from real point clouds, and (moveable) objects (Fang et al., 2020; Manivasagam et al., 2020). This idea is also implemented in HELIOS++ (Winiwarter et al., 2023) and in BLAINDER (Reitmann et al., 2021) as object "swaps". In this way, a virtual survey can be repeated over many different versions of a base scene. In BLAINDER, a single object can be replaced by another and random modifications (translation, rotation, scaling) can be applied. HELIOS++ even supports swapping and/or transforming many different scene parts at the same time. Object swaps can involve different geometry formats, e.g., a detailed mesh can be replaced by a coarse voxel model. With this functionality, researchers can easily and efficiently create simulated point clouds of a variety of scenarios, e.g., a forest in different stages of the phenological cycle or a city in different traffic and parking situations. Compared to creating completely new scenes for each epoch, this implementation is more user-friendly. Since the static parts do not have to be reloaded and previously used dynamic scene parts can be recycled, it is potentially also more efficient.

2.6.2. Scene updates during simulation run

If the scene changes during a VLS simulation run (concept of animation, cf. Section 2.4, Figure 3c), the scene must be updated with sufficient temporal resolution during a single simulation run.

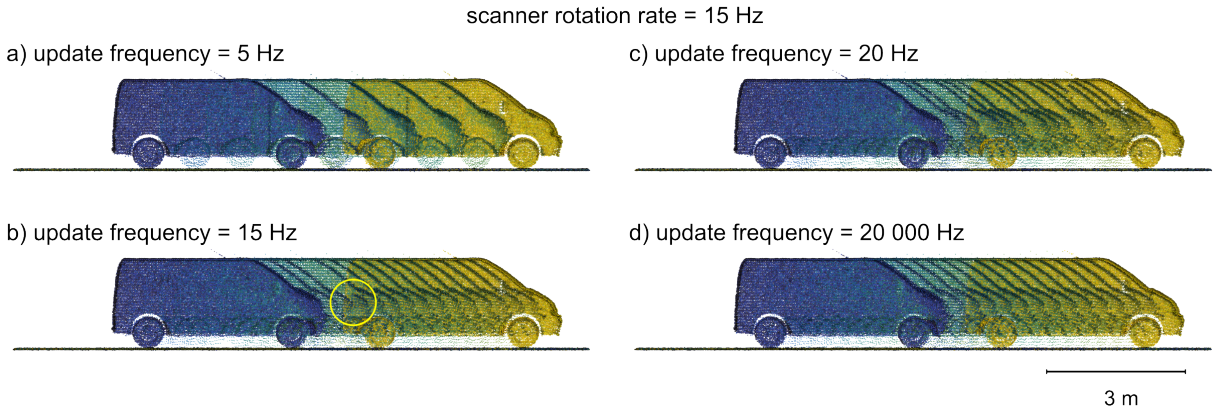

Figure 4: Mobile laser scanning example demonstrating the effect of different scene update frequencies on the resulting point clouds. A scanner model similar to the Velodyne HDL-64E is used with a rotation rate of 20 Hz and a pulse repetition frequency of 20312 Hz. The scan lasts for 3 s (simulated time) during which the ego vehicle (mounting platform) moves 15 m at 5 m/s. The scanned vehicle is static for 1 s, then moves 5 m for 1 s, then is static again for 1 s. Simulation performed with HELIOS++. Coloured by simulated time.

The combination of the LiDAR pulse frequency of the simulated sensor and the change rate of the dynamic moving object determines how frequently the scene geometry must be updated to simulate realistic point clouds. In many scenarios, motion needs to be modelled at higher rates than those used for standard movies, i.e., 24 frames per second (fps). If we assume a pulse frequency of 100 000 Hz, a scene update frequency of 24 Hz means that we only update the scene about every 4000 pulses, or - to express it in simulated time - every 1/24 seconds. This can result in point cloud patterns with visible gaps, as shown in Figure 5. For example, the VLS-4D dataset "KITTI-CARLA" was simulated with a dynamic scene update frequency of 1000 Hz and a laser frame rate, i.e., revolution or rotation frequency, of 10 Hz. Within one revolution of the laser scanner, the scene is therefore updated 100 times, simulating the "rolling shutter" effect of laser scanners (Deschaud, 2021). Synchronising scene dynamics with the frequency of the simulated laser scanner, i.e., updating the scene before each simulated LiDAR pulse, ensures high temporal realism, though it is computationally intensive.

By controlling the scene update frequency [Hz] (or the update time step [s]), the user can control the trade-off between the temporal resolution of the virtual scene and the runtime of the simulation.

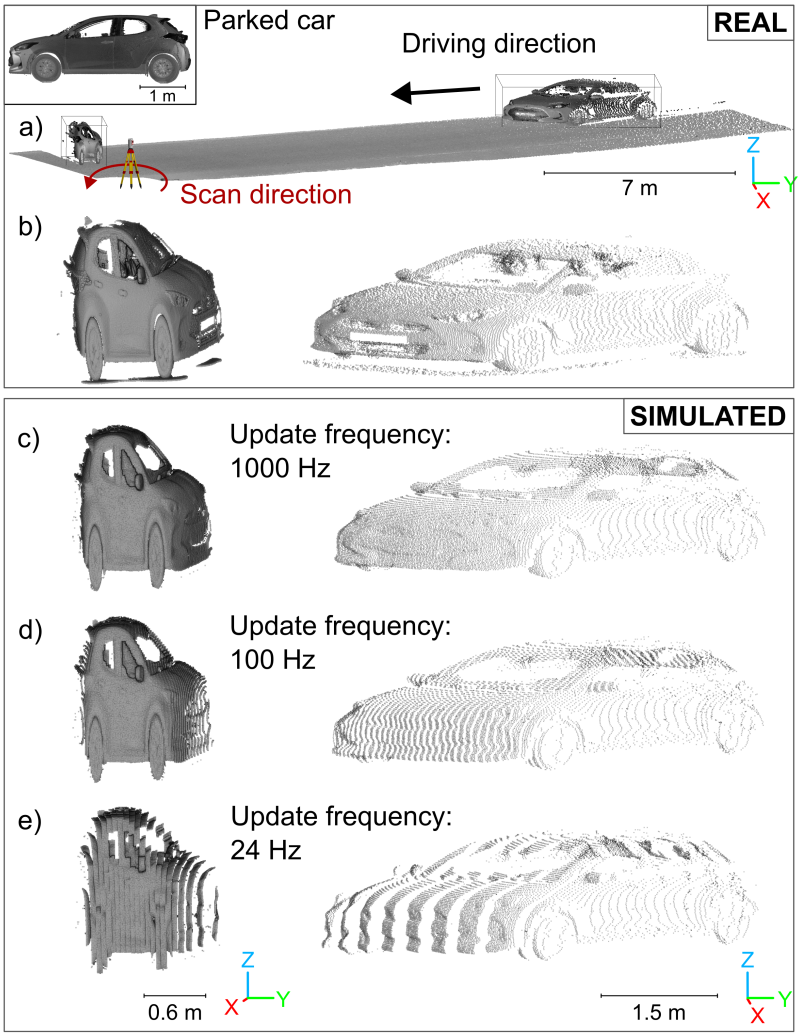

Figure 5: Terrestrial laser scanning example demonstrating the effect of different scene update frequencies on the resulting simulated point clouds using a dynamic digital twin. a) Real point cloud of a scenario where the scanner is rotating counter-clockwise while a car is approaching from the right. The car is scanned once at approximately 20 m distance, where the rotating scanner overtakes the car and a second time at approximately 2.5 m distance where the car overtakes the scanner again. This results in two distorted point cloud representations shown in b). A point cloud of a static car is shown in the top left for reference. c) – e) Simulated point clouds of a digital twin of the scenario using scene update frequencies of 1000 Hz, 100 Hz and 24 Hz. Car point clouds b – e) coloured in grey and rendered with Eye-Dome Lighting (EDL). Simulations performed with HELIOS++, version 2.0.0a3.

Figures 4 and 5 show the effect of the scene update frequency on simulated point clouds for the example of a moving car. In Figure 4, the car is scanned with a virtual Velodyne HDL-64E mounted on a mobile platform using HELIOS++. If the update frequency is less than the scanner rotation rate (Figure 4a), consecutive scanner rotations (also called "frames") capture the same version of the dynamic scene, which is not realistic. Even if the update frequency is equal to the scanner rotation rate, there can be synchronisation effects, where the scene is updated during one rotation and we see a "jump" in the point cloud (Figure 4b, yellow circle). If the update frequency is not synchronised with the scanner rotation rate, the car appears to move irregularly, even though its speed is constant (Figure 4c). For slow rotating TLS scanners, higher update frequencies are more important to avoid undesired effects like stripe patterns. Based on a real TLS acquisition with a RIEGL VZ-600i (Figure 5a), for which we built a digital twin, we demonstrate the influence of the scene update frequency. The car is driving past the scanner standing on the sidewalk in the same direction than the scanner head is rotating (rotation speed: approx. 17°/s or 0.047 Hz, pulse repetition frequency: 2200 kHz). In the resulting point cloud, the car appears twice, with different patterns of geometric distortions (Figure 5b). Panels c – e in Figure 5 show the point clouds simulated in this dynamic scenario for different scene update frequencies. Only with the update frequency of 1000 Hz (Figure 5c), no visible effects of discrete time sampling are visible.

The scenes for the experiments shown in Figures 4 and 5 were animated in Blender, converted to a HELIOS++ XML scene configuration with the add-on dyn_b2h[2], and then virtually scanned with HELIOS++ (version 2.0.0a3).

Ray tracing acceleration structures, e.g., k-dimensional tree (KDTree) or Bounding Volume Hierarchy (BVH), also need to be updated. This can be done at the same frequency as the dynamic objects or at a lower frequency.

[2] `https://github.com/3dgeo-heidelberg/dyn_b2h`, last accessed 2024-10-02

3. Current approaches

We assess the current state of VLS-4D in terms of implementation by focusing on three areas: 1) we give an overview of approaches to generate dynamic scenes, 2) we present existing LiDAR simulators, describe how they support VLS-4D and assess their fidelity, and 3) we summarise the main scientific applications of VLS-4D to date using selected publications.

3.1. Dynamic scene generation

A dynamic virtual scene is typically based on a static base scene, which can be created manually, through procedural modelling or by reconstruction from real data.

The manual creation of virtual scenes in 3D modelling software requires expertise, time and prior knowledge of the objects to be modelled. Consequently, the complexity of scenes that can be achieved by manual modelling is limited. As an alternative, procedural modelling allows the creation of complex models on a large scale by means of algorithms, i.e., in a rule-based manner, which is suitable for urban environments (Parish and Müller, 2001; Weissenberg, 2014) and vegetation (Longay et al., 2012; Stava et al., 2014; Weber and Penn, 1995). Finally, data-driven modelling refers to the generation of 3D models from real-world imagery using either photogrammetric techniques (Westoby et al., 2012) or laser-scanned point clouds.

To add the dynamics, new versions of the scene are created or the scene is animated. In the following, we will provide an overview of approaches and workflows for implementing dynamic scenes. We include examples of outdoor scenes, such as urban environments, vegetation and topographic settings.

3.1.1. Manual approaches

Manual change modelling includes the modification of scenes by adding or removing individual objects or changing their position or dimensions. This was done by de Gélis et al. (2023a) to create bi-temporal simulated point clouds of urban scenes with labelled change. With the aim of creating a pre- and post-earthquake urban dataset, Zahs et al.

(2023) used manual modelling and fracturing with the "Cell fracture" add-on[3] in Blender to model different degrees of damage to buildings.

Rigid motion animations, created by manually inserting keyframes, were used in several VLS-4D studies on object segmentation or tracking (Kumru and Ozkan, 2021; Orts-Escolano et al., 2015; Schultz et al., 2022).

3.1.2. Semi-automated approaches

Often, the aim is to automate the modelling of dynamics as several studies demonstrate. Schultz et al. (2022) partially automate dynamic scene generation by combining 1) the generation of a base scene from OpenStreetMap, 2) the insertion of objects from a model database (here from ShapeNetCore.v2; Chang et al., 2015) and 3) the addition of dynamics by exchanging geometries or implementing rigid motion via keyframes. Reitmann and Jung (2023) implemented a highly sophisticated approach to generate synthetic labelled 3D point clouds of animated fish swarms by means of sound navigation and ranging (Sonar) simulations. The authors reconstructed a static underwater environment using photogrammetry, employing data acquired through high-resolution multibeam echo sounding (underwater) as well as a camera drone (shore). Subsequently, the water body was simulated in Blender using a displacement modifier based on procedural texture noise. A rigged low-poly fish model was created and a wiggle animation was added. The swarm was then generated using a particle system. Finally, force fields were inserted to regulate the motion behaviour of the virtual fish swarm.

Wang et al. (2022) simulate plant motion for their bi-temporal synthetic test datasets by applying a nonlinear transformation function to the base meshes. Tabernig et al. (2024) reconstruct a landslide on a vegetated mountain slope by placing procedurally generated trees on a digital terrain model (DTM) computed from real data. To add the dynamics, trees are displaced along paths derived using an adaptation of the Gravitational Process Path (GPP) model (Wichmann, 2017) with different velocities.

[3] `https://docs.blender.org/manual/en/latest/addons/object/cell_fracture.html`, last accessed 2024-10-02

For modelling events such as rockfalls, physics simulation is employed, which considers aspects like gravity, friction, and collision. (Sala et al., 2019) used the "Cell fracture" add-on in Blender to subdivide a virtual rockfall source volume into many fragments for subsequent gravity-induced rockfall simulation with multi-body collision in Unity (Unity Technologies, 2024). They computed change between their pre- and post-rockfall simulation meshes by converting them to point clouds, and compared the simulated change with their reference derived from real point cloud pairs. However, the conversion from mesh to point cloud was not done with VLS.

Soil or wind erosion can be modelled using numerical models (Safonov et al., 2020). The finite element analysis software Abaqus[4] has been used in scientific studies to numerically model erosion processes of arcades and rock pillars (Safonov et al., 2020) and to model tree motion and predict mechanical strains on trees reconstructed from TLS data (Jackson et al., 2019). However, these studies were aimed at improving the understanding of environmental processes, but did not include point cloud generation with VLS.

Since trees and their dynamics are relevant for almost every animated movie or computer game (Pirk et al., 2012), several methods have been developed to generate and animate tree models. Zhao and Barbič (2013) present a system that can convert static triangular mesh plant geometry (e.g., from plant model libraries) into simulation-ready plants and that can be used as an interactive plant editor. They showcase different ways of deforming the plants: with wind, user forces and gravity. In a similar way, but focusing on tree growth rather than motion, Pirk et al. (2012) present a method to compute a developmental model from a static tree model, which allows to generate arbitrary intermediate growth stages of a tree. Such developmental models were later combined with wind simulation, allowing the simulation of both the immediate effects (tree swaying) and the long-term effects (e.g., directional growth, bud drying and abrasion) of wind influence (Pirk et al., 2014). A very comprehensive method is implemented by the software TheGrove[5], which allows to grow and animate individual trees, but also forest stands that grow together, compete for light and attenuate wind. Li

[4] `https://www.3ds.com/products/simulia/abaqus`, last accessed 2024-10-02
[5] `https://www.thegrove3d.com/`, last accessed 2024-10-02

et al. (2011) present a probabilistic approach to automatically generating realistic dynamic 3D tree models from video. A generative model can then create further similar, but not identical, trees from a single example. Since VLS studies of dynamic vegetation scenes are still rare, none of these algorithms have been combined with VLS-4D to the authors' knowledge.

Urban driving simulators like CARLA (Dosovitskiy et al., 2017) make use of traffic simulation to move vehicles and people around in the virtual environment. Vehicles can be animated so that wheels move when steering, and pedestrians are modelled as rigged actors, defined as a combination of a skin mesh and a skeleton hierarchy (Navas and Pina, 2020). Dynamic CARLA scenes have been exploited in several virtual MLS studies (Deschaud, 2021; Deschaud et al., 2021; Wang et al., 2023a). Chen et al. (2023) used the crowd simulation framework Menge (Curtis et al., 2016) together with a robotics simulator to generate VLS point cloud sequences with many moving pedestrians.

3.1.3. Data-driven approaches

In data-driven modelling, the first step is to measure or record real-world change or motion data, which is then applied to a static base model.

To model terrain erosion, Winiwarter et al. (2022a) first performed change detection and quantification on real TLS point cloud time series of an erosion-affected high-mountain slope. The derived displacement was then applied to a base mesh epoch by epoch by displacing its nodes. This way, a dynamic scene in the form of many static representations was created and different airborne laser scanning acquisition strategies for monitoring erosion could be virtually investigated (Winiwarter et al., 2022a).

Characters such as humans and animals, modelled as rigged skeletons, can be animated by transferring motion data that was captured from real living creatures. This was done in several studies to generate depth images for object detection, object tracking or pose estimation (Buys et al., 2014; Haggag et al., 2015; Vretenar and Lenac, 2015; Saleh et al., 2018; Shotton et al., 2013). Such studies can make use of openly available motion capture datasets

with diverse types of motion, e.g. the CMU Graphics Lab Motion Capture Database[6] or the KIT Whole-Body Human Motion Database[7] (Mandery et al., 2016).

Similarly, Li et al. (2013) propose to bring plants to life by mapping not only motion data onto the base meshes, but also growth information that can be derived from 4D point clouds with their algorithm.

The AdaSplats method (Richa et al., 2022) allows creation of dynamic scenes reconstructed from real data, which are not represented as triangular meshes, but as splats. To generate the SimKITTI32 dataset[8], the AdaSplats method was applied to the SemanticKITTI sequence by first splatting the static scene (without moving objects) and then extracting moving objects on each frame separately. LiDAR point clouds were then simulated using a ray-splat intersection method.

On top of that, several DL methods exist for reconstruction of 3D scenes from images and videos, which have been extended for dynamic scenes. These include works based on neural radiance fields (NeRFs, Mildenhall et al., 2020) like D-NeRF Pumarola et al., 2020), HyperNeRF (Park et al., 2021) and RoDynRF (Liu et al., 2023)), GNARF (Bergman et al., 2022)) for deforming human bodies, and k-planes (Fridovich-Keil et al.), HexPlane (Cao and Johnson, 2023) and Tensor-4D (Shao et al., 2023) which are based on feature planes for dynamic scene representation.

3.2. Existing VLS-4D simulation frameworks

Simulation software capable of explicitly handling dynamic scenes can be divided into three categories, which are summarised in Table 1.

In the following sections, we describe frameworks used in our literature review summarised in Tables 2, 3 and 4 that fall into these categories (Table 1). We only include tools that simulate LiDAR, output point clouds, and specifically support dynamic scenes, i.e., go beyond the ability of the user to run many simulations of self-extracted snapshots of dynamic scenes. Furthermore, we limit the selection to solutions that are open source.

[6] `http://mocap.cs.cmu.edu/`, last accessed 2024-10-02
[7] `https://motion-database.humanoids.kit.edu/`, last accessed 2024-10-02
[8] `https://npm3d.fr/simkitti32`, last accessed 2024-10-02

Table 1: Description of the three categories of VLS-4D simulation frameworks and selected examples of simulators which are also described throughout Section 3.2.

Category	Description	Examples
I) Standalone software	Software is explicitly developed for the purpose of LiDAR simulation.	- HELIOS++ - DyNFL
II) Plugins to 3D modelling software or game engines	LiDAR module built into widely used solutions for creating and rendering animated or interactive 3D scenes.	- BlenSor - BLAINDER - Lidar-Simulator - DeepGTAV
III) Modules of specialised robotics simulation software	The LiDAR sensor is one of many components of a complex system-level simulator.	- Gazebo - CARLA

We discuss the implementations with respect to the fidelity of the modelled ray-scene interaction, the types of dynamic scenes that can be simulated, and the configuration of the scene update frequency.

3.2.1. Standalone software

Standalone software for VLS is explicitly developed for the purpose of LiDAR simulation, typically as educational or scientific tool, and does not rely on another program to operate. Such standalone software includes comprehensive 3D radiative transfer models such as the Discrete Anisotropic Radiative Transfer (DART) model (Gastellu-Etchegorry et al., 2016; Yin et al., 2016; Yang et al., 2022). The widely used DART LiDAR model does not explicitly support dynamic scenes, but could be used with the concept of static representations or snapshots, where the user takes care of inputting modified scenes.

A well-known example for a standalone VLS framework with explicit support for dynamic scenes is the general purpose ray tracing based laser scanning simulator **HELIOS++** (Winiwarter et al., 2022b). HELIOS++ puts the focus on physically realistic modelling of the ray-scene interaction. Of the simulators discussed in this paper, it is the only one that approximates beam divergence and allows full-waveform simulations. It also returns intensity values as well as classification labels for each point and allows modelling random noise sources at various points in the simulation. However, unlike most other VLS-4D frame-

works, particularly those in category 3, it does not have its own physics engine to facilitate the animation of physically realistic object dynamics (e.g., reaction to forces and collision).

HELIOS++ explicitly supports two types of scene dynamics: Swap-on-repeat (between simulations) and rigid motions (during simulation). The swaps can be applied to any number of objects, and can include geometry swaps, geometric transformations or material changes. Rigidly moving objects can be created by assigning combinations and sequences of rigid motions to scene parts. Their temporal resolution can be set on the scene level or on the scene part level as a frequency or an absolute time step.

HELIOS++ uses a tailored KDTree data structure to speed up the ray tracing process, where a large number of ray-scene intersection checks have to be computed (Esmoris et al., 2022). This acceleration structure needs to be updated during a single simulation run when dealing with rigid motions. For efficient handling of multiple KDTrees, a so-called KDGrove is implemented. It checks if an object has changed and therefore the KDTree needs to be updated. This is done either at the same frequency as the dynamic object itself, or at a lower frequency, depending on user input.

The creation of dynamic scenes for HELIOS++ is supported by a Blender add-on[9]. This add-on converts a Blender animation into a HELIOS++-readable scene file, either as a) many static snapshots of a scene, b) a swap-on-repeat scene or b) a scene with rigid motions.

Very recently, simulation frameworks have been developed that make use of novel view synthesis such as 3D Gaussian splatting and neural fields (Richa et al., 2022; Yang et al., 2023; Wu et al., 2024).

For example, with **DyNFL** [10], Wu et al. (2024) implement neural field-based point cloud simulation of dynamic scenes for autonomous driving. They use neural scene representations generated from real LiDAR sequences and object bounding boxes to synthesise LiDAR point clouds. They divide the input 3D point cloud into a static background and a set of dynamic actors, which are each modelled as a separate neural field, following the work by Ost et al.

[9] `https://github.com/3dgeo-heidelberg/dyn_b2h`, last accessed 2024-10-02

[10] `https://github.com/prs-eth/Dynamic-LiDAR-Resimulation`, last accessed 2024-10-02

(2021). This allows scene editing, i.e., removing and inserting vehicles or changing their trajectory to create new variations of the original dynamic driving scene. DyNFL renders each intersecting neural field independently and then combines these measurements into a final point cloud using a ray drop test to account for occlusions and transparent surfaces (Wu et al., 2024).

3.2.2. Plugins to 3D modelling software or game engines

With the scene as one of the core components of VLS, it is not surprising that some popular laser scanning simulation frameworks are implemented as plug-ins to 3D modelling software or game engines. This has the advantage that scene generation and/or animation can be done in the same environment as the laser scanning simulation, and a physics engine is usually provided by the engine. 3D modelling software and game engines also often have scripting interfaces, allowing a high degree of automation.

The Blender Sensor Simulation Toolbox **BlenSor** (Gschwandtner et al., 2011) is a VLS software package directly integrated into the open-source 3D creation suite Blender (Blender Online Community, 2024). Besides examples for both a multi-channel and a single channel LiDAR device, BlenSor also simulates Time-of-flight (ToF) cameras. BlenSor allows introducing errors to the simulated LiDAR measurements using a noise model. However, simulation of the return intensity is not included.

The simulation can be used together with Blender animations, e.g., using the physics engine or armature animations, which allows for complex scenarios with changing and physically interacting scene parts. An export function for motion data of selected objects is implemented, providing the ground truth required for the validation of change analysis or object detection algorithms.

While BlenSor is a modified and stripped-down version of Blender with a more efficient ray-casting procedure directly integrated into the source code (Gschwandtner, 2012), **BLAINDER** (Neumann, 2021; Reitmann et al., 2021) is only an add-on to Blender that can simply be plugged in to an existing Blender installation with all its features. Both BlenSor and BLAINDER perform ray casting using native Blender functions. Besides

LiDAR, BLAINDER also supports Sonar (Sound Navigation and Ranging) simulation in this way.

Similar to HELIOS++, BLAINDER directly supports the simulation of dynamic scenes in two ways: Single scene part swap-on-repeat (between simulations) and animated scenes (during simulation). Besides swapping the geometry source of a single object, random modifications can be applied to the object. These include translation, rotation and scaling, which are configured by specifying upper and lower limits. For each modification, an extra simulation run will be performed (Reitmann et al., 2021). For representing changes during simulation, dynamic Blender scenes, created using keyframes or constraints or by exploiting Blender's physics simulation, can be virtually scanned with BLAINDER. Animations which are achieved through modifiers (e.g., windSway, animation modifiers) are not compatible with BLAINDER. Modifiers are applied to the scene before simulation and hence, objects with such modifiers are simply treated as static objects.

With BLAINDER, simulated point clouds can either be exported separately for each animation step (frame) or merged into a single file.

The **Lidar-Simulator** of Alldén et al. (2017)[11] is implemented in the game engine Unity (Unity Technologies, 2024), and uses the Unity physics engine for ray-casting. The dynamic objects are configured using Unity's navigation system, which works with user-defined paths, and Unity's animation system, which also allows to move the bones of pedestrians. Simulations are configured with a typical game user interface and the scene is limited to a basic terrain and a small library of static (buildings and urban furniture) and dynamic objects (vehicles and pedestrians). Simulation of the laser return intensity and ranging noise have not been considered. Alldén et al. (2017) also address the question of the appropriate number of laser shots to simulate in each physics step of the game engine, trying to find a trade-off between working memory and duration of the simulation. Overall, the focus of their work was the integration of LiDAR simulation into a game engine that provides useful tools such as the physics engine and the (real-time) visualisation of the virtual laser scanning process.

[11] `https://github.com/ptibom/Lidar-Simulator`, last accessed 2024-10-02

Finally, several studies have created simulated laser scanning data with **GTA-V**[12], a commercial open-world video game with realistic graphics set in the fictional state of San Andreas (Hurl et al., 2019; Wu et al., 2019; Yue et al., 2018; Jin et al., 2022). Since GTA-IV, Rockstar Games, Inc. employs their own game engine Rockstar Advanced Game Engine (RAGE), which uses Bullet[13] as physics engine and Euphoria (Natural Motion) to bring characters to life using Dynamic Motion Synthesis (Hardwidge, 2011; NaturalMotion Ltd., 2007; NaturalMotion, 2008).

Inspired by previous work using video games to generate ground truth semantic segmentation for synthesised in-game images, Yue et al. (2018) and Wu et al. (2019) built a LiDAR simulator into GTA-V using the **DeepGTAV** plug-in[14]. The native GTA ray casting is used to find the intersection with the scene, returning also semantic and instance labels (Yue et al., 2018). However, since the collision meshes are often simplified models, such as cylinders for pedestrians (Wu et al., 2017; Yue et al., 2018), Hurl et al. (2019) use depth buffers to generate the point clouds instead, which use more precise geometric representations. Wu et al. (2019) further enhance the simulated GTA-V based training data by using an unsupervised neural network that predicts intensity learned from real data. The GTA-V based approaches have the problem that the game engine is largely a black box and control over the simulation and especially the scene is limited.

Simulators in this category often allow for the combined synthesis of LiDAR point clouds and images. They also enable direct visualisation of the dynamic environment as well as the LiDAR process and/or the output point cloud. However, the fidelity of the LiDAR is limited by the performance of the underlying software, which is primarily designed for 3D modelling, animation, and visual effects. As a result, these frameworks have mostly been used to simulate low-cost, consumer-grade sensors. They also neglect beam divergence and therefore do not support the simulation of multiple returns or full waveforms.

[12] `https://www.rockstargames.com/de/gta-v`, last accessed 2024-10-02
[13] `https://github.com/bulletphysics/bullet3`, last accessed 2024-10-02
[14] `https://github.com/aitorzip/DeepGTAV`, last accessed 2024-10-02

3.2.3. Modules of specialised robotics simulation software

In robotics simulation frameworks, the focus is on the interactions of robots with their environment. The LiDAR sensor is only one of many components of the simulator (Gschwandtner, 2012) and is simplified due to real-time constraints. As a result, realistic noise models, reflectivity, beam divergence and full waveform are not considered and often only simple scan patterns are available.

Simulation has proven to be very useful in robotics as it provides a safe and fully controlled virtual environment for developing and testing new concepts and algorithms, and, as a more recent development, can be used for cost-efficient generation of large training datasets for ML (Choi et al., 2021). Robotics simulators are working with a physics engine such as Open Dynamics Engine (ODE) (Smith, n.d.) to solve the contact forces through which the robots interact with their environment (Farley et al., 2022). They typically have interfaces to ROS, the open-source Robot Operating System (Morgan Quigley et al., 2009), or other robotics middleware such as the Player Project (Gerkey et al., 2003).

Gazebo is a popular open-source robotics simulator that also implements simple virtual LiDAR sensors (Gerkey et al., 2003; Koenig and Howard, 2004). It supports dynamic asset loading, various sensor and noise models, and is highly extensible with custom plugins. A cloud-hosted server allows downloading and sharing of robot and scene object models, as well as virtual worlds. Dynamic objects in Gazebo can either be animated via scripts (called actors) or influenced by physics forces. A scripted animation can be a trajectory animation, a skeleton animation, or a combination of both (Open Robotics, 2024, Tutorial "Actors"). For the trajectory animation, the user provides poses that should be reached at certain points in time and Gazebo interpolates between them. For the skeleton animation, Gazebo supports the loading of animations from COLLADA (.dae) and Biovision Hierarchy (.bvh) files. The performance and temporal resolution of the simulation are the result of a combination of a) the maximum time step size of the physics engine (`max_step_size` [s]) and b) the frequency at which LiDAR data is generated (`update_frequency`) (Open Robotics, 2024).

More recently, dedicated autonomous driving simulators have emerged which include as-

set libraries of building, vehicle, and pedestrian models, pre-configured maps (or worlds) and traffic simulation. Among the most popular autonomous driving simulators is **CARLA**[15] (Dosovitskiy et al., 2017; Wang et al., 2019), an open-source software built on top of Unreal Engine[16]. CARLA simulates a dynamic world with animated vehicle and pedestrian models, and works in a server-client system. Ready-made models with animation data and attributes are available in a blueprint library and different options to define and simulate traffic scenarios are provided. CARLA LiDAR measurements are returned as packages containing all points generated during one frame interval. During this frame interval, which is defined by the frame rate (fps) of the simulation, i.e., the scene update frequency, the physics are not updated, so each measurement package is a static point cloud representation of the scene.

Based on CARLA, de la Pena et al. (2022) developed AD PerDevKit, a perception development toolkit for autonomous driving (de la Pena et al., 2022). It generates annotated LiDAR, camera and Radar data in real-time, considering only the objects in the field of view of the sensors, and publishes them to a ROS topic (i.e. a channel for communication between nodes).

3.3. Scientific Applications

Based on our literature review, we identify three main application categories, which are listed below and discussed in the following sections. For each category, we provide a tabular overview of the existing body of literature.

1. Method testing and validation (Table 2)
2. Generation of training (and testing) data for ML and DL (Table 3)
3. Investigation of data acquisition and motion effects (Table 4)

The tables summarise the studies regarding the following questions:

- What is the scientific problem that was investigated with VLS-4D?
- How were virtual dynamic scenes generated?

[15] `https://github.com/carla-simulator/carla`, last accessed 2024-10-02
[16] `https://www.unrealengine.com/`, last accessed 2024-10-02

- How were the dynamics modelled in the simulation? (change logic)
- Which simulator was used?

This revealed a multitude of scientific techniques that can be improved using VLS-4D, namely change analysis, change detection, change classification, (semantic) segmentation, (moving) object detection, dynamic object removal, pose estimation, object tracking, scene flow and scene completion (Tables 2 and 3).

3.3.1. Method validation

VLS-4D is a valuable tool for validating change analysis and change detection methods, because it incorporates virtual "ground truth" of the object positions and states at each epoch.

Bi-temporal VLS point clouds were employed to validate PlantMove, a tool for quantifying plant movement from multi-temporal point clouds (Wang et al., 2022). A dynamic scene represented by two static snapshots of a tree was scanned in both epochs, and the PlantMove motion fields were compared to the simulated motion fields, which served as true reference data. Similarly, de Gélis et al. (2021, 2023a) simulated a bi-temporal airborne laser scanning dataset for urban change detection from virtual city models. The dataset was used to compare different change detection methods.

For validating algorithms for object tracking, it is important that sequential data is used, from which the kinematics can be estimated (Kumru and Ozkan, 2021). Tabernig et al. (2024) validate different methods for tree trunk tracking using VLS-4D. They extend previous bi-temporal approaches by constructing a digital twin of a long-range permanent laser scanning (PLS) system monitoring a forested landslide. A static snapshot is extracted from their landslide animation every three hours - in simulated time - and used as input for LiDAR simulations with HELIOS++. The resulting virtual PLS time series were used to compare three methods for calculating displacement based on tree trunk detection and matching. Furthermore, using both virtual and real data, the effect of temporal scan aggregation was investigated, i.e., how merging sequential scans of PLS datasets could increase point cloud density and reduce occlusion effects, leading to higher detection rates (Tabernig

et al., 2024). Kumru and Ozkan (2021) propose a Gaussian process-based model which not only tracks objects but also estimates their shape. To generate simulated test data, they used random point sampling on geometric primitives, and mobile laser scanning simulation of moving vehicles with BlenSor.

In point clouds sensed by robotic systems under dynamic environments, the presence of dynamic objects is often a challenge for robot localisation using Simultaneous Localisation and Mapping (SLAM) algorithms. The dynamic objects decrease the SLAM point cloud registration accuracy and form ghost artefacts in resulting 3D point cloud maps which create false obstacles for path planning algorithms (Chen et al., 2023). Hence, online or offline dynamic object removal algorithms are required. Given the limited availability of annotated and sufficiently challenging (i.e., crowded) real data, virtual laser scanning sequences with dynamic objects have frequently been used for validating such algorithms (Chen et al., 2023; Fan et al., 2022; Wang et al., 2023a).

Table 2: Overview of selected publications using virtual laser scanning of dynamic scenes (VLS-4D) for method testing and validation. Scene generation is split into a) the static base scene and b) the modelling of dynamics. The table is sorted by scene change logic concept (Section 2.4). AV = autonomous vehicle, DTM = digital terrain model. GPP = Gravitational Process Path.

Method testing and validation

Targeted problem	**Scene generation**		**Change logic concept**	**Simulation framework**	**Reference**
	a) static	**b) dynamic**			
- Change analysis	Procedural tree modelling	Mesh deformation by applying nonlinear transformation function	Static representations (bi-temporal)	HELIOS++	Wang et al. (2022); PlantMove
- Change detection - Change classification	Virtual 3D city model	Manual removal, addition and modification of objects	Static representations (bi-temporal)	In-house simulator	de Gélis et al. (2021); de Gélis et al. (2023a)
- Object detection - Object tracking	DTM reconstructed from real data, procedural tree modelling	Displacement of trees using adapted GPP model	Static representations (hyper-temporal)	HELIOS++	Tabernig et al. (2024)
AV tasks, e.g. - Semantic segmentation - Object detection - Object tracking	Splatting (AdaSplats)	Frame-wise splatting of dynamic objects	Static representations (hyper-temporal)	Ray-splat ray tracing framework (OptiX)	Richa et al. (2022)
- Object tracking	Vehicle models	Rigid body animation for translation of car (U-turn)	Few static snapshots	BlenSor	Kumru and Ozkan (2021)
- Dynamic object removal	CARLA maps	Moving vehicles and rigged pedestrians, using CARLA traffic manager and blueprints	Animation within simulator	CARLA	Wang et al. (2023a) ScanTrimmer
- Dynamic object removal	GAZEBO map	Crowd simulation framework Menge	Animation within simulator	GAZEBO	Fan et al. (2022); Chen et al. (2023)

Table 2: Overview of selected publications using virtual laser scanning of dynamic scenes (VLS-4D) for method testing and validation. Scene generation is split into a) the static base scene and b) the modelling of dynamics. The table is sorted by scene change logic concept (Section 2.4). AV = autonomous vehicle, DTM = digital terrain model. GPP = Gravitational Process Path.

Method testing and validation

Targeted problem	**Scene generation**		**Change logic concept**	**Simulation framework**	**Reference**
	a) static	**b) dynamic**			
- Sensor/Robotic system validation	3D models; model database	OSI messages for dynamic object updates	Animation within simulator	LiMOX (OptiX)	Rott (2022)

3.3.2. Training data generation for machine and deep learning

There are two main motivations for using VLS-4D to generate training data for ML. First, VLS-4D can be used as a means of data permutation to create a wide range of realistic scenarios. Second, VLS-4D generates sequential data that is essential for specific tasks, such as change analysis, moving object detection or object tracking.

Synthesised RGB colour or depth images of dynamic 3D scenes have been used to train ML and DL models for object detection (for collision avoidance between cars and humans or animals), object tracking, pose estimation and body part segmentation (Buys et al., 2014; Haggag et al., 2015; Hattori et al., 2015; Marin et al., 2010; Saleh et al., 2017, 2018; Shotton et al., 2013; Mahmoud and Waslander, 2021). These studies make use of dynamic scenes to generate an abundance of realistic image training data of dynamic objects in different poses and in front of different backgrounds. Depth images were rendered with BlenSor (Saleh et al., 2017, 2018) or Blender (Buys et al., 2014), RGB images with 3DS Max (Hattori et al., 2015) or in the video games Half-Life 2 (Marin et al., 2010) and GTA-V. While only working in the image domain, these approaches have the potential to be extended to point cloud applications.

de Gélis et al. (2023b) show that for urban change classification in bi-temporal datasets, pre-training with their simulated point cloud dataset Urb3DCD–V2 significantly reduced the amount of labelled data sampled needed in the fine tuning step on real data.

Bi-temporal laser scanning data has also been simulated by Zahs et al. (2023) with HELIOS++ to train a random forest model for classification of building damage in UAV-based point clouds. A key achievement of this study was that the model trained on purely simulated bi-temporal laser scanning data performed well in predicting damage in real bi-temporal photogrammetric data, achieving a transfer between different point cloud sources.

The two urban change studies described above are both limited to two epochs, each simulated over a static representation of the urban scene (concept of few static representations, see Section 2.4).

Use of VLS-4D in the field of autonomous driving resulted in several benchmark datasets for testing and benchmarking approaches for urban object detection and segmentation (Hurl

et al., 2019; Deschaud, 2021; Deschaud et al., 2021). These datasets have been simulated using the concept of animation (see Section 2.4) in GTA-V (PreSIL; Hurl et al., 2019) and CARLA (KITTI-CARLA; Deschaud, 2021) and are provided in a format similar to the popular KITTI 3D object detection benchmark dataset[17] (Geiger et al., 2012, 2013). By supporting this format, existing tools and models developed for the KITTI dataset can be directly applied to take advantage of the simulated datasets, e.g. for transfer learning. Using a 3D object detection network (AVOD-FPN, Ku et al., 2018), Hurl et al. (2019) report a 5% improvement in average precision on the KITTI 3D Object Detection benchmark challenge[18] (Geiger et al., 2012) when pre-training with their simulated dataset before fine-tuning on the KITTI set.

Both Jabłoński et al. (2022) and de la Pena et al. (2022) generated LiDAR data with CARLA and converted the simulated LiDAR data to range images prior to training YOLO models for pedestrian detection. Jabłoński et al. (2022) compared models trained on synthetic, real and mixed datasets and achieved the highest performance with the mixed dataset. de la Pena et al. (2022) also report improved performance on real world data when real training data is supplemented with synthetic data.

Based on the work of LiDAR simulation in GTA-V by Hurl et al. (2019), GTA-SF[19], a large-scale dataset for scene flow was generated and published (Jin et al., 2022). It contains pairs of consecutive point clouds and automatic labels assigned by computing rigid motion between corresponding entities in the simulation. Jin et al. (2022) propose a mean-teacher-based domain adaptation framework to bridge the domain gap between synthetic and real-world data. Using experiments with several scene flow DL methods and real and synthetic datasets, they show that their dataset better generalises to real data than the previously introduced FlyingThings3D dataset (Mayer et al., 2016).

[17] `https://www.cvlibs.net/datasets/kitti/`, last accessed 2024-10-02

[18] `https://www.cvlibs.net/datasets/kitti/eval_object.php?obj_benchmark=3d`, last accessed 2024-10-02

[19] `https://github.com/leolyj/DCA-SRSFE`, last accessed 2024-10-02

Table 3: Overview of selected publications using virtual laser scanning of dynamic scenes (VLS-4D) for generation of training data for machine learning (ML) and deep learning (DL). Scene generation is split into a) the static base scene (if applicable) and b) the modelling of dynamics. The table is sorted by scene change logic concept (Section 2.4) and further grouped by simulation framework. GTA-V = Grand Theft Auto V, MLS = mobile laser scanning, OSI = Open Simulation Interface, OSM = OpenStreetMap.

Generation of training data for machine learning and deep learning

Targeted problem	**Scene generation a) static**	**b) dynamic**	**Change logic concept**	**Simulation framework**	**Reference**
- Change detection - Change classification	Virtual 3D city model	Manual removal, addition and modification of objects	Static representations (bi-temporal)	In-house simulator	de Gélis et al. (2021); de Gélis et al. (2023a)
- Change classification	Virtual 3D city model	Manual destruction of buildings	Static representations (bi-temporal)	HELIOS++	Zahs et al. (2023)
- Semantic segmentation	Airport model, built from OSM, object models from ShapeNetCore.v2	Object swap, change of pose (rigid motion)	Many static snapshots	BLAINDER	Schultz et al. (2022)
- Moving object detection - Semantic segmentation	Underwater environment reconstructed from real data and manual modelling	Displacement modifiers, rigged character animation, particle system, physics simulation (force field)	Single static snapshot vs. animation within simulator	Blender (sonar simulation)	Reitmann and Jung (2023)
- Object detection - Semantic segmentation	-	Video game scene (GTA-V open world)	Animation within simulator	DeepGTAV -PreSIL	Hurl et al. (2019)
- Scene flow	-	Video game scene (GTA-V open world)	Animation within simulator	DeepGTAV / DeepGTAV-PreSIL	Mahmoud and Waslander (2021)
- Scene flow	-	Video game scene (GTA-V open world)	Animation within simulator	DeepGTAV -PreSIL	Jin et al. (2022)

Table 3: Overview of selected publications using virtual laser scanning of dynamic scenes (VLS-4D) for generation of training data for machine learning (ML) and deep learning (DL). Scene generation is split into a) the static base scene (if applicable) and b) the modelling of dynamics. The table is sorted by scene change logic concept (Section 2.4) and further grouped by simulation framework. GTA-V = Grand Theft Auto V, MLS = mobile laser scanning, OSI = Open Simulation Interface, OSM = OpenStreetMap.

Generation of training data for machine learning and deep learning

Targeted problem	**Scene generation a) static**	**b) dynamic**	**Change logic concept**	**Simulation framework**	**Reference**
- Object detection - Semantic segmentation - Scene completion	CARLA maps	Moving vehicles and rigged pedestrians, using CARLA traffic manager and blueprints	Animation within simulator	CARLA	Deschaud (2021) KITTI-CARLA; Deschaud et al. (2021) Paris-CARLA
- Object detection	CARLA maps	Moving vehicles and rigged pedestrians, using CARLA traffic manager and blueprints	Animation within simulator	CARLA (AD PerDevKit)	Jabłoński et al. (2022) AD PerDevKit; de la Pena et al. (2022)
- Object detection - Semantic segmentation	Surfel-based 3D mesh from MLS data	Collection of symmetry-completed, surfel-based 3D meshes from MLS data, animated according to traffic scenarios	Animation within simulator	Ray casting + neural network for raindrop (LiDARSim)	Manivasagam et al. (2020)
- Object detection - Semantic segmentation	Neural field from MLS sequences	editable neural fields from MLS data and tracked object bounding boxes + rigid motions	Animation within simulator	Neural volume rendering from composite neural field (UniSim)	Yang et al. (2023)
- Object detection - Semantic segmentation	Neural field from MLS sequences	editable neural fields from MLS data and camera images + rigid motions	Animation within simulator	Neural volume rendering from multiple neural fields (DyNFL)	Wu et al. (2024)

3.3.3. Investigation of data acquisition and motion effects

VLS-4D can be used as a tool to investigate how the laser beam interacts with the scene and how real-world objects are represented in the scanned point clouds, depending on acquisition settings and scene dynamics (Table 4). Unlike real-world experiments, individual effects can be isolated and controlled, and reference data on the objects and their dynamics is available.

Table 4: Overview of selected publications using virtual laser scanning of dynamic scenes (VLS-4D) for investigation of data acquisition or motion effects. Scene generation is split into a) the static base scene and b) the modelling of dynamics. ALS = airborne laser scanning.

Investigation of data acquisition or motion effects

Studied effects	**Scene generation**		**Change logic concept**	**Simulation framework**	**Reference**
	a) static	**b) dynamic**			
ALS flight altitude	Virtual high-mountain slope	Transfer of displacement derived from real data to base mesh	Static representations (hyper-temporal)	HELIOS++	Winiwarter et al. (2022a)
Wind-induced tree movement	Procedural tree modelling	Leaf flutter represented by rigid motion	Animation within simulator	HELIOS++	Weiser (2024)

This makes it possible to investigate how data must be acquired in order for a method to be applicable. For instance, Winiwarter et al. (2022a) performed a simulation-based analysis to find the maximum airborne laser scanning (ALS) flight altitude at which rill erosion can be detected in a point cloud time series. To do this, they transferred known changes derived from real data to a digital twin epoch by epoch, and simulated laser scanning with different acquisition settings over all the resulting scenes. Dynamics of objects can also be visible in a single acquisition, changing the representation of objects in the point cloud by introducing blurring, distortion, or duplication of geometries. Such effects can be uncovered with VLS-4D. For example, Weiser (2024) investigates how wind-induced leaf flutter during multi-station TLS affects the accuracy of point cloud-derived metrics.

4. Challenges and Perspectives

4.1. Applications in remote sensing

To date, there are only few studies using VLS-4D for remote sensing of environment, namely for studying vegetation dynamics (Wang et al., 2022; Weiser, 2024), geomorphological processes (Tabernig et al., 2024; Winiwarter et al., 2022a) and urban change (de Gélis et al., 2023b; Zahs et al., 2023).

With the growing importance of multi-temporal data for environmental monitoring (Eitel et al., 2016), the increasing need for labelled training data for deep learning (Esmorís et al., 2024), and the frequent combination of LiDAR data from different sources (Balestra et al., 2024), VLS-4D has great potential to generate exactly these types of datasets. With known reference included, VLS-4D data can be used for training, testing and validating new methods.

Currently, more and more long-term LiDAR-based monitoring projects are emerging (Balestra et al., 2024; Campos et al., 2020; Voordendag et al., 2021). But optimising acquisition protocols and developing 4D analysis workflows should not have to wait until long time series have been captured. Instead, scientists can use digital twins of these monitoring setups and combine them with diverse change scenarios to make methodological progress much faster.

For example, VLS-4D will be useful for improving permanent monitoring of gravitational mass movements or forests, by finding optimal scan distances, acquisition intervals and sensor settings to capture the expected changes. A prototype of a digital twin of a PLS system for landslide monitoring was already presented by (Tabernig et al., 2024).

Taking the work by Reitmann and Jung (2023) as an example, modelling techniques such as particle systems in combination with VLS-4D could also enable simulations for counting and monitoring bird, bat or insect swarms.

Finally, as shown by Weiser (2024) for leaf flutter, VLS-4D helps to understand the ways in which object motion affects their point cloud representations and influences the point cloud metrics we derive from them. This knowledge can be used to develop algorithms

to correct for such motion effects, or to quantify motion, interpret it and use it as proxy for object properties. The significant effects of leaf angle dynamics on satellite-derived vegetation indices have been demonstrated by Kattenborn et al. (2024). They did not use LiDAR simulation, but performed reflectance simulations with the radiative transfer model PROSAIL (Jacquemoud et al., 2009), comparing scenarios with static and dynamic leaf angle distributions. Future VLS-4D studies can build on these methods and findings.

Our literature review revealed that there are already many VLS-4D studies in the field of robotics and autonomous driving. They use VLS-4D to support method development for tasks such as object detection, object tracking, scene flow or dynamic object removal. Hence, many technical solutions for dynamic scene generation, animation and point cloud rendering already exist, and the transfer of these methods to LiDAR-based Earth observation should be pushed forward.

4.2. Realism

From our comparison of simulation frameworks in Section 3.2, we found that there is currently no solution that combines all three change logic concepts (Section 2.4) and all ways to implement scene animation (Section 2.5) with sophisticated and realistic laser beam modelling (i.e., support of full-waveform modelling). In the VLS-4D frameworks based on 3D modelling software and game engines, complex animations (e.g., character animation, physics-based animation, particle animation) are possible, but scan patterns, intensity computation and noise models are usually simplified and beam divergence is completely neglected. HELIOS++ as a standalone general-purpose LiDAR simulation software supports many scan patterns, models beam divergence, and can compute the full waveform, but the dynamics are limited to rigid motions and scene part swaps. For character animation, physics-based animations and morphing, static 3D snapshots taken from animations with external software must be used as a workaround. Future efforts should focus on combining realistic beam modelling and ray tracing with complex 3D animation.

The biggest challenge in VLS-4D remains the same as for VLS of static scenes: the reality gap between real and simulated data. On the one hand, VLS-4D can be a means to close this

gap by incorporating scene dynamics instead of neglecting them. On the other hand, VLS-4D adds additional complexity to VLS by including the temporal dimension. In addition to conventional VLS components (such as scene geometries, material properties, scan patterns, beam divergence, multiple returns, and sensor noise), VLS-4D requires realistic modelling of the type, speed and resolution of scene dynamics (cf. Section 2.6 and Figures 4 and 5). If the dynamics are not modelled in a suitable way, VLS-4D point clouds may be even less realistic than their conventional static VLS counterparts.

Several studies have shown that there is a consistent performance gap between models trained on real data and models trained on simulated VLS-4D data alone (Jin et al., 2022 for scene flow estimation, Hurl et al., 2019, de la Pena et al., 2022 and Jabłoński et al., 2022 for object detection, Manivasagam et al., 2020 for segmentation and object detection). At present, the combination of VLS-4D data with real data is more promising. In the meantime, different strategies for domain adaptation can be used to handle the domain shift (e.g., Jin et al., 2022). In addition, more studies are needed that thoroughly analyse the realism and fitness-for-use of the simulated data, e.g., by comparing it with real data obtained in controlled lab experiments. Such experiments can also help to find good trade-offs between computational demands and realism, e.g., by finding out what scene update frequencies are needed to model specific phenomena.

For realistic scene modelling and animation, VLS-4D already uses advanced methods from 3D computer animation, including character animation and physics simulation. Beyond this, VLS-4D may also benefit from state-of-the-art AI-based methods such as neural network-based generative models for character animation (Holden et al., 2020).

4.3. Ray tracing vs. neural network-based rendering

A novel alternative to traditional ray tracing for point cloud simulation are Neural Radiance Fields (NeRFs; Mildenhall et al., 2020). Several NeRF extensions have been developed, such as Dynamic NeRFs (D-NeRFs; Pumarola et al., 2020), for non-rigid geometries, and Neural LiDAR Fields (NFL; Huang et al., 2023), which incorporate LiDAR principles into the neural field framework, taking into account beam divergence and multiple returns. The

frameworks UniSim (Yang et al., 2023) and DyNFL (Wu et al., 2024) already implement neural field-based point cloud simulation of dynamic scenes (i.e., VLS-4D) for the autonomous driving domain.

The reliance of these neural field-based approaches on real laser scanning data for scene generation can be seen as both a strength and a weakness. On the one hand, using real data alleviates the need for costly manual scene generation and ensures realism of the overall context. On the other hand, resources for data acquisition and pre-processing (e.g., object detection and bounding box tracking as necessary for DyNFL) are needed, the scenarios are restricted to the environments of captured real scenes, and quality aspects of the input point cloud affect the scene representations.

4.4. Computing performance

Existing solutions for VLS-4D (Section 3.2) suffer from memory constraints and long computation times, which limits the scope of possible applications.

VLS-4D has two computationally intensive components: scene updates and the ray-scene interaction (typically ray tracing). The computational cost of scene updates increases with the number of dynamic geometric primitives, the complexity of their dynamics and the frequency of updates. A systematic comparison of the contribution of each of these aspects is needed. This would allow to identify the best optimisation strategies for a given survey and application.

Several strategies can be used to improve memory usage and reduce computation time, which we discuss in the following.

Since dynamic objects within a single scene may change at different rates, have different relevance, or be located at different distances from the scanner, one strategy is to adapt the resolution of the individual scene dynamics and scene geometries to the survey characteristics. In terms of scene dynamics, important scene parts may be animated with higher temporal resolution, which requires that the simulator supports different update frequencies for different scene parts (cf. HELIOS++). In terms of scene geometry, background objects can be modelled at a coarser resolution and foreground objects at a higher resolution. This

resolution can also change dynamically over (simulation) time, depending on the scanner position in the scene. In computer graphics, this is known as the well-known concept of Level of Detail (LOD, Clark, 1976). When rendering a scene, progressively less detailed representations are used for distant, small or unimportant parts of the scene (Luebke, 2003, Chapter 1).

Regarding the scene update strategy, the computational performance of VLS-4D can be improved by updating a) only those objects that change, b) only at the times they change, and c) only if they are in the scanner's field of view (FOV) at those times. Thus, a smart LiDAR simulator will avoid computing expensive scene updates for objects that are outside the FOV.

To accurately model the beam divergence, a typical approach is to approximate the laser beam cone using subrays. This significantly increases the number of ray-scene intersections that have to be computed, making efficient ray-tracing even more important. Ray tracing is usually accelerated using structures such as a KDTree (e.g., HELIOS++; Esmoris et al., 2022) or a BVH (e.g., Blender-based frameworks and OptiX; Parker et al., 2010). As suggested by Parker et al. (2010), efficiency can be increased by creating separate acceleration structures for static and dynamic regions of a scene. Acceleration structures in the NVIDIA OptiX ray tracing engine can be of different types, meaning that high-quality static acceleration structures can be combined with dynamically updated acceleration structures in a single scene (Parker et al., 2010). HELIOS++ uses only KDTrees as a search structure, but builds a single tree for all static objects combined, and separate trees for each dynamic object. HELIOS++ also allows object-specific frequencies for checking whether the KDTree of a dynamic object needs to be updated. Only if the respective object has changed, the KDTree is updated.

5. Conclusion

Virtual laser scanning (VLS) has proven to be an extremely useful tool for survey planning, method development and training data generation. At the same time, VLS for environmental science has almost exclusively been performed in a single epoch over a static

scene. As a result, environmental dynamics such as forest growth and geomorphological surface change have been neglected.

However, due to the increasing importance of environmental monitoring, the emergence of multi-temporal datasets and the need for large amounts of informative training data, VLS research needs to be extended to dynamic scenes (VLS-4D). VLS-4D incorporates reference data not only on the semantics but also of the dynamics of objects in the scene. Obtaining such data with sufficient accuracy in the real world is usually not feasible or even impossible. Hence, VLS-4D provides unique opportunities to uncover links between object properties and their point cloud representations.

In this review, we have provided a theoretical framework of VLS-4D. After defining VLS-4D, we identified characteristics of dynamic scenes and animation strategies to represent them. We present three scene change logic concepts with which VLS-4D can be implemented: a) few static representations, where the entire scene or individual scene objects are swapped, b) many static snapshots, typically sampled consecutively from an animation, and c) animation within the simulator, where the scene is updated during the simulation. The third concept in particular requires specialised VLS-4D software. We identified the main use cases of VLS-4D as the development and validation of new methods, the generation of training data for ML, and the investigation of data acquisition and motion effects.

While VLS-4D is already becoming a standard in the field of autonomous driving, existing technical solutions for both dynamic scene generation and compatible LiDAR simulation still need to be transferred and adapted to environmental monitoring.

Looking into technical implementations of VLS-4D, we found standalone LiDAR simulators, plugins to 3D modelling software, and submodules of specialised robotics software, but no solution combines all three change logic concepts with complex scene animation and realistic laser beam modelling (e.g., including multi-target capabilities). Hence, different existing technical implementations need to be combined to allow realistic high-fidelity LiDAR simulation of dynamic environments like forests or active landslides, which differ from already frequently studied urban traffic scenarios.

Once this is achieved, VLS-4D has the potential to reduce or even eliminate the typical

time lag between the release cycles of new sensor systems and datasets and the development of suitable data analysis workflows. Instead of waiting for new data to be acquired before developing and adapting methods, this can be done much earlier by using LiDAR simulations with novel sensor configurations or acquisition workflows. This is particularly relevant for time series data, where it may take years or decades until the dataset is complete.

Acknowledgements

The graphical abstract and Figures 1, 2 and 3 have been designed using resources from Flaticon.com (Graphical Abstract: Concept and plane icon by Iconjam; configuration/AI icon and drone by Freepik; smart car icon by PIXARTIST. Figure 1: Plane icon by Iconjam; drone by Freepik; smart car icon by PIXARTIST. Figure 2: Shift icon by Flowicon; digital twin, drone, interaction, scale, speed, tripod and wave icons by Freepik; probability icon by IconBaander; timeline icon by juicy_fish; color icon by nawicon; deformation icon by PLANBSTUDIO; scale icon by Smartline, area icon by Smashicons; path icon by VectorPortal. Figure 3: animation icon by gravisio).

Scenes shown in Figures 1, 2 and 3 have been rendered in Blender.

We thank William Albert and Ronald Tabernig for their support with data acquisition for the car experiment and Ronald Tabernig for his helpful comments on the manuscript.

Funding

This research was funded by the Deutsche Forschungsgemeinschaft (DFG, German Research Foundation) – no. 496418931 (VirtuaLearn3D) and no. 528521476 (Fostering a community-driven and sustainable HELIOS++ scientific software) – and by the Federal Ministry of Education and Research (BMBF) – no. 02WDG1696 (AIMon 5.0) – within the funding measure "Digital GreenTech – Environmental Engineering meets Digitalisation" as part of the "Research for Sustainability" (FONA) Strategy.

Author contribution

Hannah Weiser: Conceptualisation, Investigation, Visualisation, Writing - Original Draft, Writing - Reviewing and Editing. **Bernhard Höfle**: Conceptualisation, Funding acquisition, Supervision, Writing - Reviewing and Editing.

Data availability

The input data for the LiDAR simulations and the resulting point clouds used to create the figures will be made available via the institutional repository for Open Research Data from Heidelberg University upon acceptance (preliminary link for reviewers: https://heibox.uni-heidelberg.de/d/59d388069dae4ed98e8d/).

References

Alldén, T., Chemander, M., Davar, S., Jansson, J., Laurenius, R., Tibom, P., 2017. Virtual Generation of LiDAR Data for Autonomous Vehicles. B.Sc. thesis. University of Gothenburg, Chalmers University of Technology. Gothenburg, Sweden. URL: http://publications.lib.chalmers.se/records/fulltext/251700/251700.pdf.

Balestra, M., Marselis, S., Sankey, T.T., Cabo, C., Liang, X., Mokroš, M., Peng, X., Singh, A., Stereńczak, K., Vega, C., Vincent, G., Hollaus, M., 2024. Lidar data fusion to improve forest attribute estimates: A review. Current Forestry Reports 10, 281–297. doi:10.1007/s40725-024-00223-7.

Bechtold, S., Höfle, B., 2016. HELIOS: A multi-purpose lidar simulation framework for research, planning and training of laser scanning operations with airborne, ground-based mobile and stationary platforms. ISPRS Annals of the Photogrammetry, Remote Sensing and Spatial Information Sciences III-3, 161–168. doi:10.5194/isprsannals-III-3-161-2016.

Behley, J., Garbade, M., Milioto, A., Quenzel, J., Behnke, S., Stachniss, C., Gall, J., 2019. SemanticKITTI: A dataset for semantic scene understanding of LiDAR sequences, in: Proc. of the IEEE/CVF International Conf. on Computer Vision (ICCV). doi:10.48550/arXiv.1904.01416.

Bergman, A.W., Kellnhofer, P., Yifan, W., Chan, E.R., Lindell, D.B., Wetzstein, G., 2022. Generative neural articulated radiance fields, in: NeurIPS. URL: https://proceedings.neurips.cc/paper_files/paper/2022/file/7dbafa7d2051218f364c9a38ef1150de-Paper-Conference.pdf, doi:10.48550/arXiv.2206.14314.

Blain, J.M., 2022. The Complete Guide to Blender Graphics Computer Modeling & Animation. A K Peters/CRC Press, Boca Raton. doi:10.1201/9781003226420.

Blender Documentation Team, 2024. Blender 4.0 reference manual. URL: https://docs.blender.org/manual/en/4.0/. last accessed 2024-02-29.

Blender Online Community, 2024. Blender - a 3D modelling and rendering package. Blender Foundation. URL: http://www.blender.org.

Buys, K., Cagniart, C., Baksheev, A., de Laet, T., de Schutter, J., Pantofaru, C., 2014. An adaptable system for RGB-D based human body detection and pose estimation. Journal of Visual Communication and Image Representation 25, 39–52. doi:10.1016/j.jvcir.2013.03.011.

Campos, M.B., Litkey, P., Wang, Y., Chen, Y., Hyyti, H., Hyyppä, J., Puttonen, E., 2020. A long-term terrestrial laser scanning measurement station to continuously monitor structural and phenological dynamics of boreal forest canopy. Frontiers in plant science 11, 606752. doi:10.3389/fpls.2020.606752.

Cao, A., Johnson, J., 2023. Hexplane: A fast representation for dynamic scenes. CVPR .

Chang, A.X., Funkhouser, T., Guibas, L., Hanrahan, P., Huang, Q., Li, Z., Savarese, S., Savva, M., Song, S., Su, H., Xiao, J., Yi, L., Yu, F., 2015. ShapeNet: An Information-Rich 3D Model Repository. Technical Report arXiv:1512.03012 [cs.GR]. Stanford University — Princeton University — Toyota Technological Institute at Chicago.

Chen, Z., Zhang, K., Chen, H., Wang, M.Y., Zhang, W., Yu, H., 2023. DORF: A dynamic object removal framework for robust static LiDAR mapping in urban environments. IEEE Robotics and Automation Letters 8, 7922–7929. doi:10.1109/LRA.2023.3323196.

Choi, H., Crump, C., Duriez, C., Elmquist, A., Hager, G., Han, D., Hearl, F., Hodgins, J., Jain, A., Leve, F., Li, C., Meier, F., Negrut, D., Righetti, L., Rodriguez, A., Tan, J., Trinkle, J., 2021. On the use of simulation in robotics: Opportunities, challenges, and suggestions for moving forward. Proceedings of the National Academy of Sciences of the United States of America 118. doi:10.1073/pnas.1907856118.

Chopine, A., 2012. 3D Art Essentials. 1st edition ed., Focal press, Oxford, UK.

Clark, J.H., 1976. Hierarchical geometric models for visible surface algorithms. Communications of the ACM 19, 547–554. doi:10.1145/360349.360354.

Curtis, S., Best, A., Manocha, D., 2016. Menge: A modular framework for simulating crowd movement. Collective Dynamics 1. doi:10.17815/CD.2016.1.

de la Pena, J., Bergasa, L.M., Antunes, M., Arango, F., Gomez-Huelamo, C., Lopez-Guillen, E., 2022. AD PerDevKit: An autonomous driving perception development kit using CARLA simulator and ROS, in: 2022 IEEE 25th International Conference on Intelligent Transportation Systems (ITSC), IEEE. pp. 4095–4100. doi:10.1109/ITSC55140.2022.9922369.

Deschaud, J.E., 2021. KITTI-CARLA: a KITTI-like dataset generated by CARLA simulator. arXiv e-prints URL: https://doi.org/10.48550/arXiv.2109.00892.

Deschaud, J.E., Duque, D., Richa, J.P., Velasco-Forero, S., Marcotegui, B., Goulette, F., 2021. Paris-

CARLA-3D: A real and synthetic outdoor point cloud dataset for challenging tasks in 3D mapping. Remote Sensing 13, 4713. doi:10.3390/rs13224713.

Dosovitskiy, A., Ros, G., Codevilla, F., Lopez, A., Koltun, V., 2017. CARLA: An open urban driving simulator, in: Proceedings of the 1st Annual Conference on Robot Learning, pp. 1–16. URL: https://proceedings.mlr.press/v78/dosovitskiy17a/dosovitskiy17a.pdf.

Eitel, J.U., Höfle, B., Vierling, L.A., Abellán, A., Asner, G.P., Deems, J.S., Glennie, C.L., Joerg, P.C., LeWinter, A.L., Magney, T.S., Mandlburger, G., Morton, D.C., Müller, J., Vierling, K.T., 2016. Beyond 3-D: The new spectrum of LiDAR applications for earth and ecological sciences. Remote Sensing of Environment 186, 372–392. doi:10.1016/j.rse.2016.08.018.

Erleben, K., Sporring, J., Henriksen, K., Dohlmann, H., 2005. Physics-based Animation. Graphics Series, Charles River Media. URL: https://iphys.wordpress.com/wp-content/uploads/2020/01/erleben.ea05.pdf.

Esmorís, A.M., Weiser, H., Winiwarter, L., Cabaleiro, J.C., Höfle, B., 2024. Deep learning with simulated laser scanning data for 3d point cloud classification. ISPRS Journal of Photogrammetry and Remote Sensing 215, 192–213. doi:10.1016/j.isprsjprs.2024.06.018.

Esmoris, A.M., Yermo, M., Weiser, H., Winiwarter, L., Hofle, B., Rivera, F.F., 2022. Virtual LiDAR simulation as a high performance computing challenge: Toward HPC HELIOS++. IEEE Access 10, 105052–105073. doi:10.1109/ACCESS.2022.3211072.

Fan, T., Shen, B., Chen, H., Zhang, W., Pan, J., 2022. DynamicFilter: an online dynamic objects removal framework for highly dynamic environments, in: 2022 International Conference on Robotics and Automation (ICRA), IEEE. pp. 7988–7994. doi:10.1109/ICRA46639.2022.9812356.

Fang, J., Zhou, D., Yan, F., Zhao, T., Zhang, F., Ma, Y., Wang, L., Yang, R., 2020. Augmented LiDAR simulator for autonomous driving. IEEE Robotics and Automation Letters 5, 1931–1938. doi:10.1109/LRA.2020.2969927.

Farley, A., Wang, J., Marshall, J.A., 2022. How to pick a mobile robot simulator: A quantitative comparison of CoppeliaSim, Gazebo, MORSE and Webots with a focus on accuracy of motion. Simulation Modelling Practice and Theory 120, 102629. doi:10.1016/j.simpat.2022.102629.

Fridovich-Keil, S., Meanti, G., Warburg, F., Recht, B., Kanazawa, A., . K-planes: Explicit radiance fields in space, time, and appearance. doi:10.48550/arXiv.2301.10241.

Gastellu-Etchegorry, J.P., Yin, T., Lauret, N., Grau, E., Rubio, J., Cook, B.D., Morton, D.C., Sun, G., 2016. Simulation of satellite, airborne and terrestrial lidar with dart (i): Waveform simulation with quasi-monte carlo ray tracing. Remote Sensing of Environment 184, 418–435. doi:10.1016/j.rse.2016.07.010.

Gaydon, C., Daab, M., Roche, F., 2024. FRACTAL: An ultra-large-scale aerial lidar dataset for 3D semantic segmentation of diverse landscapes. doi:10.48550/arXiv.2405.04634.

Geiger, A., Lenz, P., Stiller, C., Urtasun, R., 2013. Vision meets robotics: The KITTI dataset. The International Journal of Robotics Research 32, 1231–1237. doi:10.1177/0278364913491297.

Geiger, A., Lenz, P., Urtasun, R., 2012. Are we ready for autonomous driving? the KITTI vision benchmark suite, in: 2012 IEEE Conference on Computer Vision and Pattern Recognition, IEEE. pp. 3354–3361. doi:10.1109/CVPR.2012.6248074.

de Gélis, I., Lefèvre, S., Corpetti, T., 2021. Change detection in urban point clouds: An experimental comparison with simulated 3D datasets. Remote Sensing 13, 2629. doi:10.3390/rs13132629.

de Gélis, I., Lefèvre, S., Corpetti, T., 2023a. Siamese KPConv: 3D multiple change detection from raw point clouds using deep learning. ISPRS Journal of Photogrammetry and Remote Sensing 197, 274–291. doi:10.1016/j.isprsjprs.2023.02.001.

de Gélis, I., Saha, S., Shahzad, M., Corpetti, T., Lefèvre, S., Zhu, X.X., 2023b. Deep unsupervised learning for 3D ALS point clouds change detection. ISPRS Open Journal of Photogrammetry and Remote Sensing 9, 100044. doi:10.1016/j.ophoto.2023.100044.

Gerkey, B., Vaughan, R.T., Howard, A., 2003. The player/stage project: Tools for multi-robot and distributed sensor systems, in: Proceedings of the 11th International Conference on Advanced Robotics (ICAR 2003). Coimbra, Portugal, pp. 317–232.

Gschwandtner, M., 2012. Support Framework for Obstacle Detection on Autonomous Trains. Phd thesis. University of Salzburg. Salzburg. URL: https://download.blensor.org/gschwandtner12b.pdf.

Gschwandtner, M., Kwitt, R., Uhl, A., Pree, W., 2011. BlenSor: Blender sensor simulation toolbox, in: Bebis, G., Boyle, R., Parvin, B., Koracin, D., Wang, S., Kyungnam, K., Benes, B., Moreland, K., Borst, C., DiVerdi, S., Yi-Jen, C., Ming, J. (Eds.), Advances in Visual Computing. Springer Berlin Heidelberg, Berlin, Heidelberg. volume 6939 of *Lecture Notes in Computer Science*, pp. 199–208. doi:10.1007/978-3-642-24031-7_20.

Hackel, T., Savinov, N., Ladicky, L., Wegner, J.D., Schindler, K., Pollefeys, M., 2017. SEMANTIC3D.NET: A new large-scale point cloud classification benchmark, in: ISPRS Annals of the Photogrammetry, Remote Sensing and Spatial Information Sciences, pp. 91–98.

Haggag, H., Hossny, M., Nahavandi, S., Haggag, S., Creighton, D., 2015. Body parts segmentation with attached props using RGB-D imaging, in: 2015 International Conference on Digital Image Computing: Techniques and Applications (DICTA), IEEE. pp. 1–8. doi:10.1109/DICTA.2015.7371243.

Hardwidge, B., 2011. Bullet physics – the future of GPU-accelerated physics? URL: https://www.bit-tech.net/reviews/tech/graphics/amd-manju-hegde-gaming-physics/3/.

Hattori, H., Boddeti, V.N., Kitani, K., Kanade, T., 2015. Learning scene-specific pedestrian detectors without real data, in: 2015 IEEE Conference on Computer Vision and Pattern Recognition (CVPR), IEEE. pp. 3819–3827. doi:10.1109/CVPR.2015.7299006.

Holden, D., Kanoun, O., Perepichka, M., Popa, T., 2020. Learned motion matching. ACM Transactions on Graphics 39. doi:10.1145/3386569.3392440.

Huang, S., Gojcic, Z., Wang, Z., Williams, F., Kasten, Y., Fidler, S., Schindler, K., Litany, O., 2023. Neural lidar fields for novel view synthesis, in: 2023 IEEE/CVF International Conference on Computer Vision (ICCV), IEEE. pp. 18190–18200. doi:10.1109/ICCV51070.2023.01672.

Hurl, B., Czarnecki, K., Waslander, S., 2019. Precise synthetic image and LiDAR (PreSIL) dataset for autonomous vehicle perception, in: 2019 IEEE Intelligent Vehicles Symposium (IV), IEEE. pp. 2522–2529. doi:10.1109/IVS.2019.8813809.

Jabłoński, P., Iwaniec, J., Zabierowski, W., 2022. Comparison of pedestrian detectors for LiDAR sensor trained on custom synthetic, real and mixed datasets. Sensors (Basel, Switzerland) 22. doi:10.3390/s22187014.

Jackson, T., Shenkin, A., Wellpott, A., Calders, K., Origo, N., Disney, M., Burt, A., Raumonen, P., Gardiner, B., Herold, M., Fourcaud, T., Malhi, Y., 2019. Finite element analysis of trees in the wind based on terrestrial laser scanning data. Agricultural and Forest Meteorology 265, 137–144. doi:10.1016/j.agrformet.2018.11.014.

Jacquemoud, S., Verhoef, W., Baret, F., Bacour, C., Zarco-Tejada, P.J., Asner, G.P., François, C., Ustin, S.L., 2009. PROSPECT+SAIL models: A review of use for vegetation characterization. Remote Sensing of Environment 113, S56–S66. doi:10.1016/j.rse.2008.01.026.

Jin, Z., Lei, Y., Akhtar, N., Li, H., Hayat, M., 2022. Deformation and correspondence aware unsupervised synthetic-to-real scene flow estimation for point clouds, in: 2022 IEEE/CVF Conference on Computer Vision and Pattern Recognition (CVPR), IEEE. pp. 7223–7233. doi:10.1109/CVPR52688.2022.00709.

Kattenborn, T., Wieneke, S., Montero, D., Mahecha, M.D., Richter, R., Guimarães-Steinicke, C., Wirth, C., Ferlian, O., Feilhauer, H., Sachsenmaier, L., Eisenhauer, N., Dechant, B., 2024. Temporal dynamics in vertical leaf angles can confound vegetation indices widely used in earth observations. Communications Earth & Environment 5. doi:10.1038/s43247-024-01712-0.

Kharroubi, A., Poux, F., Ballouch, Z., Hajji, R., Billen, R., 2022. Three dimensional change detection using point clouds: A review. Geomatics 2, 457–485. doi:10.3390/geomatics2040025.

Koenig, N., Howard, A., 2004. Design and use paradigms for gazebo, an open-source multi-robot simulator, in: 2004 IEEE/RSJ International Conference on Intelligent Robots and Systems (IROS) (IEEE Cat. No.04CH37566), IEEE. pp. 2149–2154. doi:10.1109/IROS.2004.1389727.

Ku, J., Mozifian, M., Lee, J., Harakeh, A., Waslander, S.L., 2018. Joint 3D proposal generation and object detection from view aggregation, in: 2018 IEEE/RSJ International Conference on Intelligent Robots and Systems (IROS), IEEE. pp. 1–8. doi:10.1109/IROS.2018.8594049.

Kumru, M., Ozkan, E., 2021. Three-dimensional extended object tracking and shape learning using gaussian

processes. IEEE Transactions on Aerospace and Electronic Systems 57, 2795–2814. doi:10.1109/TAES.2021.3067668.

Kölle, M., Laupheimer, D., Schmohl, S., Haala, N., Rottensteiner, F., Wegner, J.D., Ledoux, H., 2021. The Hessigheim 3D (H3D) benchmark on semantic segmentation of high-resolution 3D point clouds and textured meshes from UAV LiDAR and multi-view-stereo. ISPRS Open Journal of Photogrammetry and Remote Sensing 1, 11. doi:https://doi.org/10.1016/j.ophoto.2021.100001.

Li, C., Deussen, O., Song, Y.Z., Willis, P., Hall, P., 2011. Modeling and generating moving trees from video, in: Proceedings of the 2011 SIGGRAPH Asia Conference, ACM, New York, NY, USA. pp. 1–12. doi:10.1145/2024156.2024161.

Li, Y., Fan, X., Mitra, N.J., Chamovitz, D., Cohen-Or, D., Chen, B., 2013. Analyzing growing plants from 4D point cloud data. ACM Transactions on Graphics 32, 1–10. doi:10.1145/2508363.2508368.

Liu, C.j., Liu, Z., Chai, Y.j., Liu, T.t., 2020. Review of virtual traffic simulation and its applications. Journal of Advanced Transportation 2020, 1–9. doi:10.1155/2020/8237649.

Liu, Y.L., Gao, C., Meuleman, A., Tseng, H.Y., Saraf, A., Kim, C., Chuang, Y.Y., Kopf, J., Huang, J.B., 2023. Robust dynamic radiance fields, in: 2023 IEEE/CVF Conference on Computer Vision and Pattern Recognition (CVPR), IEEE. pp. 13–23. doi:10.1109/CVPR52729.2023.00010.

Lohani, B., Khan, P., Kumar, V., Gupta, S., 2024. Role of simulated lidar data for training 3d deep learning models: An exhaustive analysis. Journal of the Indian Society of Remote Sensing doi:10.1007/s12524-024-01905-2.

Lohani, B., Mishra, R., 2007. Generating LiDAR data in laboratory: LiDAR simulator. Int. Arch. Photogramm. Remote Sens. 52, 161–168. URL: https://isprs-annals.copernicus.org/articles/III-3/161/2016/isprs-annals-III-3-161-2016.pdf.

Longay, S., Runions, A., Boudon, F., Prusinkiewicz, P., 2012. TreeSketch: Interactive procedural modeling of trees on a tablet. doi:10.2312/SBM/SBM12/107-120.

Luebke, D.P., 2003. Level of detail for 3D graphics. The Morgan Kaufmann series in computer graphics and geometric modeling. first edition ed., Morgan Kaufmann Publishers, Estados Unidos.

Mahmoud, A., Waslander, S.L., 2021. Sequential fusion via bounding box and motion pointpainting for 3D objection detection, in: 2021 18th Conference on Robots and Vision (CRV), IEEE. pp. 9–16. doi:10.1109/CRV52889.2021.00013.

Mandery, C., Terlemez, O., Do, M., Vahrenkamp, N., Asfour, T., 2016. Unifying representations and large-scale whole-body motion databases for studying human motion. IEEE Transactions on Robotics 32, 796–809. doi:10.1109/TRO.2016.2572685.

Manivasagam, S., Wang, S., Wong, K., Zeng, W., Sazanovich, M., Tan, S., Yang, B., Ma, W.C., Urtasun, R., 2020. LiDARsim: Realistic LiDAR simulation by leveraging the real world, in: 2020 IEEE/CVF

Conference on Computer Vision and Pattern Recognition (CVPR), IEEE. pp. 11164–11173. doi:10.1109/CVPR42600.2020.01118.

Marin, J., Vazquez, D., Geronimo, D., Lopez, A.M., 2010. Learning appearance in virtual scenarios for pedestrian detection, in: 2010 IEEE Computer Society Conference on Computer Vision and Pattern Recognition, IEEE. pp. 137–144. doi:10.1109/CVPR.2010.5540218.

Mayer, N., Ilg, E., Hausser, P., Fischer, P., Cremers, D., Dosovitskiy, A., Brox, T., 2016. A large dataset to train convolutional networks for disparity, optical flow, and scene flow estimation, in: IEEE Computer Society, Institute of Electrical and Electronics Engineers, Inc. (Eds.), Proceedings, 29th IEEE Conference on Computer Vision and Pattern Recognition (CVPR), IEEE. pp. 4040–4048. doi:10.1109/CVPR.2016.438.

Mildenhall, B., Srinivasan, P.P., Tancik, M., Barron, J.T., Ramamoorthi, R., Ng, R., 2020. NeRF: Representing scenes as neural radiance fields for view synthesis, in: Vedaldi, A., Bischof, H., Brox, T., Frahm, J.M. (Eds.), Computer Vision – ECCV 2020. Springer International Publishing, Cham. volume 12346 of *Lecture Notes in Computer Science*, pp. 405–421. doi:10.1007/978-3-030-58452-8{\textunderscore}24.

Morgan Quigley, Brian Gerkey, Ken Conley, Josh Faust, Tully Foote, Jeremy Leibs, Eric Berger, Rob Wheeler, Andrew Ng, 2009. ROS: an open-source robot operating system, in: "Proc. of the IEEE Intl. Conf. on Robotics and Automation (ICRA) Workshop on Open Source Robotics", "Kobe, Japan".

NaturalMotion, 2008. Frequently asked questions. URL: https://web.archive.org/web/20100103165025/http://naturalmotion.com/faq.htm.

NaturalMotion Ltd., 2007. NaturalMotion and rockstar games, inc. announce development partnership: Upcoming next-generation titles to utilize euphoria motion synthesis engine. URL: https://web.archive.org/web/20070927213342/http://www.naturalmotion.com/files/nm_rockstar_2007.pdf. press release.

Navas, D., Pina, B., 2020. Pedestrians and their implementation. URL: https://www.youtube.com/watch?v=Uoz2ihDwaWA.

Neumann, L., 2021. BLAINDER. URL: https://github.com/ln-12/blainder-range-scanner.

Open Robotics, 2024. Docs / gazebo harmonic. URL: https://gazebosim.org/docs. last accessed 2024-06-04.

Orts-Escolano, S., Garcia-Rodriguez, J., Morell, V., Cazorla, M., Saval, M., Azorin, J., 2015. Processing point cloud sequences with growing neural gas, in: 2015 International Joint Conference on Neural Networks (IJCNN), IEEE / Institute of Electrical and Electronics Engineers Incorporated. pp. 1–8. doi:10.1109/IJCNN.2015.7280709.

Ost, J., Mannan, F., Thuerey, N., Knodt, J., Heide, F., 2021. Neural scene graphs for dynamic scenes, in: 2021 IEEE/CVF Conference on Computer Vision and Pattern Recognition (CVPR), IEEE. pp. 2855–

2864. doi:10.1109/CVPR46437.2021.00288.

Parish, Y.I.H., Müller, P., 2001. Procedural modeling of cities, in: Pocock, L. (Ed.), Proceedings of the 28th annual conference on Computer graphics and interactive techniques, ACM, New York, NY, USA. pp. 301–308. doi:10.1145/383259.383292.

Park, K., Sinha, U., Hedman, P., Barron, J.T., Bouaziz, S., Goldman, D.B., Martin-Brualla, R., Seitz, S.M., 2021. Hypernerf: A higher-dimensional representation for topologically varying neural radiance fields. ACM Transactions on Graphics 40.

Parker, S.G., Bigler, J., Dietrich, A., Friedrich, H., Hoberock, J., Luebke, D., McAllister, D., McGuire, M., Morley, K., Robison, A., Stich, M., 2010. OptiX: a general purpose ray tracing engine. ACM Transactions on Graphics 29, 1–13. doi:10.1145/1778765.1778803.

Pirk, S., Niese, T., Deussen, O., Neubert, B., 2012. Capturing and animating the morphogenesis of polygonal tree models. ACM Transactions on Graphics 31, 169:1–169:10. doi:10.1145/2366145.2366188.

Pirk, S., Niese, T., Hädrich, T., Benes, B., Deussen, O., 2014. Windy trees. ACM Transactions on Graphics 33, 1–11. doi:10.1145/2661229.2661252.

Puliti, S., Pearse, G., Surový, P., Wallace, L., Hollaus, M., Wielgosz, M., Astrup, R., 2023. For-instance: a uav laser scanning benchmark dataset for semantic and instance segmentation of individual trees. arXiv:2309.01279.

Pumarola, A., Corona, E., Pons-Moll, G., Moreno-Noguer, F., 2020. D-nerf: Neural radiance fields for dynamic scenes, in: Proceedings of the IEEE/CVF Conference on Computer Vision and Pattern Recognition. doi:10.48550/arXiv.2011.13961.

Reitmann, S., Jung, B., 2023. Generating synthetic labeled data of animated fish swarms in 3D worlds with particle systems and virtual sound wave sensors, in: Arseniev, D.G., Aouf, N. (Eds.), Cyber-Physical Systems and Control II. Springer International Publishing, Cham. volume 460 of *Lecture Notes in Networks and Systems*, pp. 131–140. doi:10.1007/978-3-031-20875-1_12.

Reitmann, S., Neumann, L., Jung, B., 2021. BLAINDER-a blender ai add-on for generation of semantically labeled depth-sensing data. Sensors (Basel, Switzerland) 21. doi:10.3390/s21062144.

Reynolds, C.W., 1999. Steering behaviors for autonomous characters, in: Proceedings of Game Developers Conference, San Francisco, California. pp. 763–782.

Richa, J.P., Deschaud, J.E., Goulette, F., Dalmasso, N., 2022. AdaSplats: Adaptive splatting of point clouds for accurate 3d modeling and real-time high-fidelity lidar simulation. Remote Sensing 14, 6262. doi:10.3390/rs14246262.

Rott, R., 2022. Dynamic update of stand-alone LiDAR model based on ray tracing using the nvidia optix engine, in: 2022 International Conference on Connected Vehicle and Expo (ICCVE), IEEE. pp. 1–6. doi:10.1109/ICCVE52871.2022.9743000.

Safonov, A., Filippi, M., Mašín, D., Bruthans, J., 2020. Numerical modeling of the evolution of arcades and rock pillars. Geomorphology 365, 107260. doi:10.1016/j.geomorph.2020.107260.

Sala, Z., Hutchinson, D.J., Harrap, R., 2019. Simulation of fragmental rockfalls detected using terrestrial laser scans from rock slopes in south-central british columbia, canada. Natural Hazards and Earth System Sciences 19, 2385–2404. doi:10.5194/nhess-19-2385-2019.

Saleh, K., Hossny, M., Hossny, A., Nahavandi, S., 2017. Cyclist detection in LiDAR scans using faster r-cnn and synthetic depth images, in: 2017 IEEE 20th International Conference on Intelligent Transportation Systems (ITSC), IEEE. pp. 1–6. doi:10.1109/ITSC.2017.8317599.

Saleh, K., Hossny, M., Nahavandi, S., 2018. Effective vehicle-based kangaroo detection for collision warning systems using region-based convolutional networks. Sensors (Basel, Switzerland) 18. doi:10.3390/s18061913.

Schultz, M., Reitmann, S., Jung, B., Alam, S., 2022. Towards automated apron operations - training of neural networks for semantic segmentation using synthetic LiDAR sensors, in: 2022 Winter Simulation Conference (WSC), IEEE. pp. 418–429. doi:10.1109/WSC57314.2022.10015391.

Shao, R., Zheng, Z., Tu, H., Liu, B., Zhang, H., Liu, Y., 2023. Tensor4d: Efficient neural 4d decomposition for high-fidelity dynamic reconstruction and rendering.

Shotton, J., Girshick, R., Fitzgibbon, A., Sharp, T., Cook, M., Finocchio, M., Moore, R., Kohli, P., Criminisi, A., Kipman, A., Blake, A., 2013. Efficient human pose estimation from single depth images. IEEE transactions on pattern analysis and machine intelligence 35, 2821–2840. doi:10.1109/TPAMI.2012.241.

Smith, R.L., n.d. Open dynamics engine (ode). URL: http://ode.org/.

Stava, O., Pirk, S., Kratt, J., Chen, B., Měch, R., Deussen, O., Benes, B., 2014. Inverse procedural modelling of trees. Computer Graphics Forum 33, 118–131. doi:10.1111/cgf.12282.

Tabernig, R., Albert, W., Weiser, H., Rutzinger, M., Höfle, B., 2024. Investigating the effects of temporal aggregation of permanent laser scanning data on landslide monitoring in forested areas. URL: https://heibox.uni-heidelberg.de/f/84410adad9cf47fd8951/. in Preparation.

Unity Technologies, 2024. Unity. URL: https://unity.com/. Game development platform.

Voordendag, A.B., Goger, B., Klug, C., Prinz, R., Rutzinger, M., Kaser, G., 2021. Automated and permanent long-range terrestrial laser scanning in a high mountain environment: Setup and first results. ISPRS Annals of the Photogrammetry, Remote Sensing and Spatial Information Sciences V-2-2021, 153–160. doi:10.5194/isprs-annals-V-2-2021-153-2021.

Vretenar, L., Lenac, K., 2015. People tracking using synthetically generated depth maps, in: 2015 38th International Convention on Information and Communication Technology, Electronics and Microelectronics (MIPRO), IEEE. pp. 646–651. doi:10.1109/MIPRO.2015.7160352.

Wang, D., Puttonen, E., Casella, E., 2022. PlantMove: A tool for quantifying motion fields of plant

movements from point cloud time series. International Journal of Applied Earth Observation and Geoinformation 110, 102781. doi:10.1016/j.jag.2022.102781.

Wang, F., Zhuang, Y., Gu, H., Hu, H., 2019. Automatic generation of synthetic LiDAR point clouds for 3-D data analysis. IEEE Transactions on Instrumentation and Measurement 68, 2671–2673. doi:10.1109/TIM.2019.2906416.

Wang, J., Duan, Y., Ji, J., 2023a. ScanTrimmer: an online dynamic objects removal framework in laser scan for robust localization, in: 2023 IEEE International Conference on Robotics and Biomimetics (ROBIO), IEEE. pp. 1–6. doi:10.1109/ROBIO58561.2023.10354661.

Wang, Z., Zhang, Y., Luo, L., Yang, K., Xie, L., 2023b. An end-to-end point-based method and a new dataset for street-level point cloud change detection. IEEE Transactions on Geoscience and Remote Sensing 61, 1–15. doi:10.1109/TGRS.2023.3295386.

Weber, J., Penn, J., 1995. Creation and rendering of realistic trees, in: Proceedings of the 22nd annual conference on Computer graphics and interactive techniques, pp. 119–128.

Weiser, H., 2024. How Does Vegetation Movement During Laser Scanning Affect Common Point Cloud-Derived Metrics? A Virtual Laser Scanning Study. M.Sc. thesis. Heidelberg University. Heidelberg. doi:10.11588/heidok.00035451.

Weissenberg, J., 2014. Inverse Procedural Modelling and Applications. Phd thesis. ETH Zurich. Zurich. URL: https://www.varcity.ethz.ch/paper/phd2014_weissenberg_thesis.pdf.

Westoby, M.J., Brasington, J., Glasser, N.F., Hambrey, M.J., Reynolds, J.M., 2012. 'structure-from-motion' photogrammetry: A low-cost, effective tool for geoscience applications. Geomorphology 179, 300–314. doi:10.1016/j.geomorph.2012.08.021.

Wichmann, V., 2017. The gravitational process path (GPP) model (v1.0) – a GIS-based simulation framework for gravitational processes. Geoscientific Model Development 10, 3309–3327. doi:10.5194/gmd-10-3309-2017.

Winiwarter, L., Anders, K., Schröder, D., Höfle, B., 2022a. Virtual laser scanning of dynamic scenes created from real 4D topographic point cloud data. ISPRS Annals of the Photogrammetry, Remote Sensing and Spatial Information Sciences V-2-2022, 79–86. doi:10.5194/isprs-annals-V-2-2022-79-2022.

Winiwarter, L., Esmorís Pena, A.M., Weiser, H., Anders, K., Martínez Sánchez, J., Searle, M., Höfle, B., 2022b. Virtual laser scanning with HELIOS++: A novel take on ray tracing-based simulation of topographic full-waveform 3D laser scanning. Remote Sensing of Environment 269, 112772. doi:10.1016/j.rse.2021.112772.

Winiwarter, L., Esmorís Pena, A.M., Yermo García, M., Martínez Sánchez, J., Searle, M., Weiser, H., Anders, K., Höfle, B., 2023. helios: Heidelberg LiDAR Operations Simulator ++ (HELIOS++). URL: https://github.com/3dgeo-heidelberg/helios/.

Wu, B., Wan, A., Yue, X., Keutzer, K., 2017. SqueezeSeg: Convolutional neural nets with recurrent CRF for real-time road-object segmentation from 3D LiDAR point cloud. doi:10.48550/arXiv.1710.07368.

Wu, B., Zhou, X., Zhao, S., Yue, X., Keutzer, K., 2019. SqueezeSegV2: Improved model structure and unsupervised domain adaptation for road-object segmentation from a LiDAR point cloud, in: 2019 International Conference on Robotics and Automation (ICRA), IEEE. pp. 4376–4382. doi:10.1109/ICRA.2019.8793495.

Wu, H., Zuo, X., Leutenegger, S., Litany, O., Schindler, K., Huang, S., 2024. Dynamic lidar re-simulation using compositional neural fields, in: The IEEE Conference on Computer Vision and Pattern Recognition (CVPR). URL: https://shengyuh.github.io/dynfl/assets/DyNFL.pdf, doi:10.48550/arXiv.2312.05247.

Xu, M.L., Jiang, H., Jin, X.G., Deng, Z., 2014. Crowd simulation and its applications: Recent advances. Journal of Computer Science and Technology 29, 799–811. doi:10.1007/s11390-014-1469-y.

Yang, S., Li, T., Gong, X., Peng, B., Hu, J., 2020. A review on crowd simulation and modeling. Graphical Models 111, 101081. doi:10.1016/j.gmod.2020.101081.

Yang, X., Wang, Y., Yin, T., Wang, C., Lauret, N., Regaieg, O., Xi, X., Gastellu-Etchegorry, J.P., 2022. Comprehensive lidar simulation with efficient physically-based dart-lux model (i): Theory, novelty, and consistency validation. Remote Sensing of Environment 272, 112952. doi:10.1016/j.rse.2022.112952.

Yang, Z., Chen, Y., Wang, J., Manivasagam, S., Ma, W.C., Yang, A.J., Urtasun, R., 2023. Unisim: A neural closed-loop sensor simulator, in: 2023 IEEE/CVF Conference on Computer Vision and Pattern Recognition (CVPR), IEEE. pp. 1389–1399. doi:10.1109/CVPR52729.2023.00140.

Yin, T., Lauret, N., Gastellu-Etchegorry, J.P., 2016. Simulation of satellite, airborne and terrestrial lidar with dart (ii): Als and tls multi-pulse acquisitions, photon counting, and solar noise. Remote Sensing of Environment 184, 454–468. doi:10.1016/j.rse.2016.07.009.

Yue, X., Wu, B., Seshia, S.A., Keutzer, K., Sangiovanni-Vincentelli, A.L., 2018. A LiDAR point cloud generator: from a virtual world to autonomous driving, in: Aizawa, K., Lew, M., Satoh, S. (Eds.), Proceedings of the 2018 ACM on International Conference on Multimedia Retrieval, ACM, New York, NY, USA. pp. 458–464. doi:10.1145/3206025.3206080.

Zahs, V., Anders, K., Kohns, J., Stark, A., Höfle, B., 2023. Classification of structural building damage grades from multi-temporal photogrammetric point clouds using a machine learning model trained on virtual laser scanning data. International Journal of Applied Earth Observation and Geoinformation 122, 103406. doi:10.1016/j.jag.2023.103406.

Zhao, Y., Barbič, J., 2013. Interactive authoring of simulation-ready plants. ACM Transactions on Graphics 32, 1–12. doi:10.1145/2461912.2461961.